ASIA-PACIFIC NETWORK FOR
GLOBAL CHANGE RESEARCH

ARCP Final Report

Project Reference Number: ARCP2015-03CMY-Li

Assessing Spatiotemporal Variability of NPP, NEP and Carbon Sinks of Global Grassland Ecosystem in Response to Climate Change in 1911-2011

The following collaborators worked on this project:

1. **Prof. Jianlong Li,** The Global Change Research Institute in Nanjing University, China; jili2008@nju.edu.cn
2. **Prof. Renchin Tsolmon,** Remote Sensing and GIS Lab., Research Center for Geophysics, National Project University of Mongolia, Mongolia; tzr112@psu.edu
3. **Prof. Muhammad Mohsin Iqbal,** Global Change Impact Studies Centre (GCISC), Pakistan; mohsin.iqbal@gcisc.org.pk
4. **Prof. Alim Salimovich Pulatov**, Eco-GIS Centre, Trashkent Institute of Irrigation and Melioration in Uzbekistan; alimpulatov@mail.ru

Table of Content

Project Overview

Project Duration	:	2013 -2017
Funding Awarded	:	US$ 40,000 for Year 1; US$ 36,000 for Year 2; US$25,200 for Year 3
Key organisations involved	:	1. Prof. Jianlong Li The Global Change Research Institute in Nanjing University, China; jili2008@nju.edu.cn 2. Prof. Renchin Tsolmon Remote Sensing and GIS Lab., Research Center for Geophysics, National Project University of Mongolia, Mongolia; tzr112@psu.edu 3. Prof. Muhammad Mohsin Iqbal Global Change Impact Studies Centre (GCISC), Pakistan; mohsin.iqbal@gcisc.org.pk 4. Prof. Alim Salimovich Pulatov Eco-GIS Centre, Tashkent Institute of Irrigation and Melioration in Uzbekistan; alimpulatov@mail.ru

Project Summary

The project addressed existing gaps in the field of global land use and climate change research. It focused on building and enhancing scientific capacity in three developing countries and explored the quantifying methods on assessing spatiotemporal variability of net primary production (NPP), NEP and carbon sinks of global grassland ecosystem in response to climate change and human activity during 1911-2011. This is a new attempt to integrate natural and social sciences in the study of land use change and climate change, and to overcome critical gaps in knowledge on how to enhance and manage the global grassland ecosystem, which includes management of grassland production, biomass, NPP, NEP, and carbon sinks and environmental goals, in the face of climate change in the period 1911-2011.

Keywords: climate change, Human activities, comprehensive sequential classification system (CSCS), global grassland ecosystems, NPP, NEP, Carbon Sinks; Grassland degradation; Quantitative assessment using comprehensive methods.

Project outputs and outcomes

Project outputs:

1. Two APN training-workshops in Nanjing University and in Inner Mongolia

- A training workshop and international meeting was held in Nanjing University from 29 May – 2 June 2013, and were attended by 36 students and 10 lecturers from the four collaborating countries.
- Two training workshop and international meeting were held in Xilinhot City on 25-29 June 2014 and attended by a total of 56 persons from four countries.

2. Workshops and field surveys in the study sites (Inner-Mongolia and Xinjiang)
3. Participation in MAIRS conference in Beijing, China
   - Ten (10) young scientists and lecturers participated in the MAIRS Conference in Beijing, China on April 7-12, 2014.
4. Final workshop, summarizing the project, was organised in Beijing, China, on 8-10 April 2017.
5. Assessment results of variations of distribution, extent and NPP of global natural vegetation in response to climate change in 1911-2000.
6. Grassland ecosystem model BEPS-GESS and its synthetical application on carbon cycling study on Temperate Eurasian Steppe (Apendix1-2).

Potential for further work

1. Due to the limited financial support obtained from APN, a large amount of in-kind data, models and resources were not able to be utilised in the development of the tool and field case study applications.
2. Some of the case study applications are still in progress and need additional resources to complete. The methodology, model and reviewing system developed in this project has broad applicability in more countries.
3. One of the potential future scientific researches is to expand the methodology and model to incorporate related issues such as husbandry and farm.
4. For wider use of the integrated system and results, it is highly important to develop good user-interface and technical and user guides.

Main Publications in 2013-2017

1. Yang, Y., Wang, Z., Li, J., Gang, C., Zhang, Y., Odeh, I., & Qi, J. (2017). Assessing the spatiotemporal dynamic of global grassland carbon use efficiency in response to climate

change from 2000 to 2013. Acta Oecologica, 81, 22–31. https://doi.org/10.1016/j.actao.2017.04.004

2. Wang, Z., Yang, Y., Li, J., Zhang, C., Chen, Y., Wang, K., Qi, J. (2017). Simulation of terrestrial carbon equilibrium state by using a detachable carbon cycle scheme. Ecological Indicators, 75, 82–94. https://doi.org/10.1016/j.ecolind.2016.12.014
3. Gang, C., Zhang, Y., Wang, Z., Chen, Y., Yang, Y., Li, J., Odeh, I. (2017). Modeling the dynamics of distribution, extent, and NPP of global terrestrial ecosystems in response to future climate change. Global and Planetary Change, 148, 153–165. https://doi.org/10.1016/j.gloplacha.2016.12.007
4. Chen, Y., Mu, S., Sun, Z., Gang, C., Li, J., Padarian, J., Li, S. (2016). Grassland Carbon Sequestration Ability in China: A New Perspective from Terrestrial Aridity Zones. Rangeland Ecology & Management, 69(1), 84–94. http://doi.org/10.1016/j.rama.2015.09.003
5. Wang, Z., Zhang, Y., Yang, Y., Zhou, W., Gang, C., Zhang, Y., Qi, J. (2016). Quantitative assess the driving forces on the grassland degradation in the Qinghai–Tibet Plateau, in China. Ecological Informatics, 33, 32–44. https://doi.org/10.1016/j.ecoinf.2016.03.006
6. Yang, Y., Wang, Z., Li, J., Gang, C., Zhang, Y., Zhang, Y., Qi, J. (2016). Comparative assessment of grassland degradation dynamics in response to climate variation and human activities in China, Mongolia, Pakistan and Uzbekistan from 2000 to 2013. Journal of Arid Environments, 135, 164–172. https://doi.org/10.1016/j.jaridenv.2016.09.004
7. Zhang, Y., Zhang, C., Wang, Z., Chen, Y., Gang, C., An, R., & Li, J. (2016). Vegetation dynamics and its driving forces from climate change and human activities in the Three-River Source Region, China from 1982 to 2012. Science of The Total Environment, 563–564, 210–220. https://doi.org/10.1016/j.scitotenv.2016.03.223
8. Gang, C., Wang, Z., Zhou, W., Chen, Y., Li, J., Chen, J., Groisman, P. Y. (2015). Assessing the Spatiotemporal Dynamic of Global Grassland Water Use Efficiency in Response to Climate Change from 2000 to 2013. Journal of Agronomy and Crop Science, n/a-n/a. http://doi.org/10.1111/jac.12137
9. Gang, C., Zhou, W., Wang, Z., Chen, Y., Li, J., Chen, J., Groisman, P. Y. (2015). Comparative Assessment of Grassland NPP Dynamics in Response to Climate Change in China, North America, Europe and Australia from 1981 to 2010. Journal of Agronomy and Crop Science, 201(1), 57–68. http://doi.org/10.1111/jac.12088
10. Gang, C., Wang, Z., Zhou, W., Chen, Y., Li, J., Cheng, J., Chen, C. (2015). Projecting the dynamics of terrestrial net primary productivity in response to future climate change under

the RCP2.6 scenario. Environmental Earth Sciences, 74(7), 5949–5959. http://doi.org/10.1007/s12665-015-4618-x

11. Gang, C., Zhou, W., Li, J., Chen, Y., Mu, S., Ren, J., Groisman, P. Y. (2013). Assessing the spatiotemporal variation in distribution, extent and NPP of terrestrial ecosystems in response to climate change from 1911 to 2000. PLoS ONE, 8(11), e80394. doi:10.1371/journal.pone.0080394
12. Mu, S. J., Chen, Y. Z., Li, J. L., Ju, W. M., Odeh, I. O. A., & Zou, X. L. (2013). Grassland dynamics in response to climate change and human activities in Inner Mongolia, China between 1985 and 2009. The Rangeland Journal, 35(3), 315–329.
13. Mu, S., Zhou, S., Chen, Y., Li, J., Ju, W., & Odeh, I. O. A. (2013). Assessing the impact of restoration-induced land conversion and management alternatives on net primary productivity in Inner Mongolian grassland, China. Global and Planetary Change, 108, 29–41. doi:10.1016/j.gloplacha.2013.06.007
14. Sun, Z., Sun, C., Zhou, W., Ju, W., & Li, J. (2013). Evaluating the net primary productivity in the grasslands of southern China from 2001 to 2010 using a new land portfolio assessment model. Plant Ecology, 214(10), 1223–1232. doi:10.1007/s11258-013-0246-2
15. Wang, Z., Gang, C., Li, X., Chen, Y., & Li, J. (2015). Application of a normalized difference impervious index (NDII) to extract urban impervious surface features based on Landsat TM images. International Journal of Remote Sensing, 1–15. http://doi.org/10.1080/01431161.2015.1007250
16. Yang, H., Gang, C., Mu, S., Zhang, C., Zhou, W., & Li, J. (2014). Jin 10 nian Xinjiang caodi shengtai xitong jing chuji shengchanli ji qi shikong geju bianhua yanjiu [Analysis of the spatiotemporal variation in net primary productivity of grassland during the past 10 years in Xinjiang]. Acta Prataculturae Sinica, 23(3), 39–50. doi:10.11686/cyxb20140305
17. Yizhao, C., Jianyang, X., Zhengguo, S., Jianlong, L., Yiqi, L., Chengcheng, G., & Zhaoqi, W. (2015). The role of residence time in diagnostic models of global carbon storage capacity: model decomposition based on a traceable scheme. Scientific Reports, 5, 16155. http://doi.org/10.1038/srep16155
18. Zhou, W., Gang, C., Zhou, F., Li, J., Dong, X., & Zhao, C. (2015). Quantitative assessment of the individual contribution of climate and human factors to desertification in northwest China using net primary productivity as an indicator. Ecological Indicators, 48, 560–569. http://doi.org/10.1016/j.ecolind.2014.08.043

19. Zhou, W., Gang, C., Chen, Y., Mu, S., Sun, Z., & Li, J. (2014). Grassland coverage inter-annual variation and its coupling relation with hydrothermal factors in China during 1982–2010. Journal of Geographical Sciences, 24(4), 593–611. doi:10.1007/s11442-014-1108-0
20. Zhou, W., Gang, C., Li, J., Zhang, C., Mu, S., & Sun, Z. (2014). 1982-2010 nian Zhongguo caodi fugaidu de shikong dongtai ji qi dui qihou bianhua de xiangying [Spatial-temporal dynamics of grassland coverage and its response to climate change in China during 1982-2010]. Journal of Geographical Sciences, 69(1), 15–30. doi:10.11821/dlxb201401002
21. Zhou, W., Gang, C., Zhou, L., Chen, Y., Li, J., Ju, W., & Odeh, I. (2014). Dynamic of grassland vegetation degradation and its quantitative assessment in the northwest China. Acta Oecologica, 55, 86–96. doi:10.1016/j.actao.2013.12.006
22. Zhou, W., Li, J. L., Mu, S. J., Gang, C. C., & Sun, Z. G. (2013). Effects of ecological restoration-induced land-use change and improved management on grassland net primary productivity in the Shiyanghe River Basin, north-west China. Grass and Forage Science, n/a–n/a. doi:10.1111/gfs.12073
23. Zhou, W., Sun, Z., Li, J., Gang, C., & Zhang, C. (2013). Desertification dynamic and the relative roles of climate change and human activities in desertification in the Heihe River Basin based on NPP. Journal of Arid Land, 5(4), 465–479. doi:10.1007/s40333-013-0181-z

Acknowledgments

This work was supported by the Asia Pacific Network for Global Change Research (APN) (ARCP2015-03CMY-Li). We also thank the China Meteorological Data Sharing Service System for providing climate datasets and data derives from each meteorological station. We thank Prof. Jizhou Ren from Lanzhou University for his guidance on the method, Prof. Jingming Chen from Nanjing University and Prof. Jiaguo Qi from The Center for Global Change & Earth Observations, Michigan State University, East Lansing, USA, for their guidance on this work. We also appreciate the NOAA and The Oak Ridge National Laboratory Distributed Active Archive Canter (ORNL DAAC) for sharing data sets. We also appreciate the CRU and NOAA for sharing datasets.

1. Introduction

Grasslands ecosystem, one of the world's important ecosystem types, accounts for nearly 40 % of the world's land surface. It has important adjustment effects on terrestrial ecosystem function, especially to global terrestrial carbon cycle process. Additionally, grassland ecosystem is quite sensitive to global climate change. Moreover, it has been deeply influenced by climate change and human activities for food production and animal husbandry development. However, at present the response mechanism and correlation between grassland and environment factors are not clear and large uncertainties still exist in estimating grassland carbon storage and its response to climate change, such as the response of grassland structure, function and carbon cycle to climate change and human activities, especially to grazing intervention. In particular, the area of global grassland area, grassland types, grassland productivity, and grassland carbon storage etc. are not quite sure. Additionally, researches about issues mentioned above are relative rare compared with other ecosystems, and there are many blank areas, which need to be explored and studied.

In order to solve the above scientific problems and to illuminate the responses of grassland ecosystem function and carbon storage in response to climate, we will do the following researches to complete the above research tasks (see Figure 1).

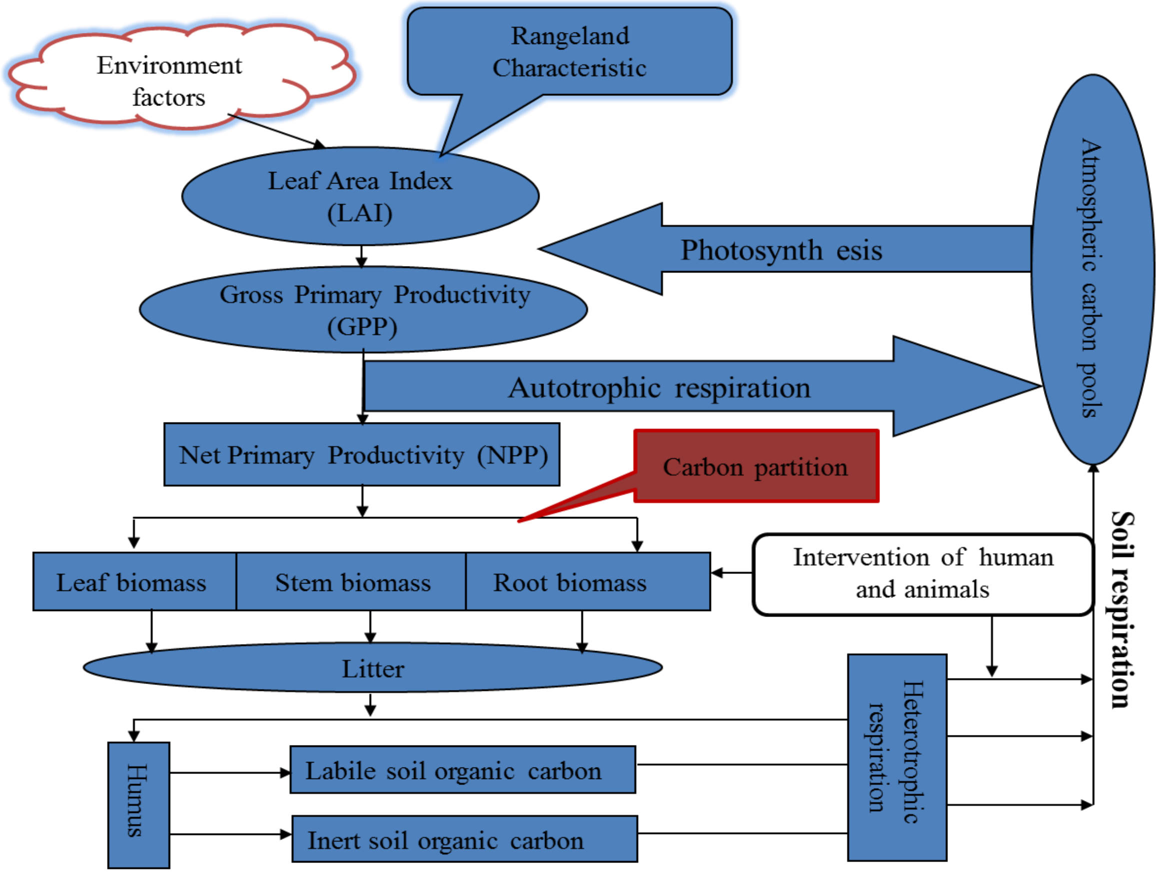

Figure 1 Grassland ecosystem carbon cycle process schematic diagram.

Vegetation classification models play an important role in studying the response of the terrestrial ecosystem to global climate change. Additionally, with the progress of technology and the advanced needs of grassland production and management in human society, scholars from home and abroad posed a variety of grassland classification methods, such as Holdridge Life Zone (HLZ) and BIOME4 potential natural vegetation. We designed the CSCS (Comprehensive and Sequential

Classification System) method based on thermal and water index, the global grassland types were classified and the grassland areas and productivity were calculated of different grassland types. The CSCS model designed by ourselves based on four factors, putting the class as the basic unit. Advantage of the method is to bring the various types of grassland isolated in the world into a unified classification system, and breaking the historical limitation of independent named regions of different grassland types in the world (Akiyama & Kawamura, 2007; Chen, et al., 2014; Fan, et al., 2012; Foley & Pollard, 2000; French, 1979; Gang, et al., 2014; Gao, et al., 2013; Han, et al., 2008; Herrmann, Anyamba, & Tucker, 2005; Horion, Cornet, Erpicum, & Tychon, 2013; Intergovernmental Panel on Climate Change, 2014; Li, 1997; Lieth, 1975; Lieth & Box, 1972; Liu & Zha, 2004; Lu, Batistella, Mausel, & Moran, 2007; Ma, Zhou, & Pei, 2012; Mu, et al., 2013; Mu, et al., 2013; O'Mara, 2012).

2. Methodology

2.1. CSCS classify methods of vegetation from our team

In practice, the class is determined by combining the quantitative biological climate indices of average annual cumulative temperature above 0°C (Σθ) (i.e., Growing Degree-Days on 0°C base, GDD0) and humidity index (K), as calculated by the following formula (Akiyama & Kawamura, 2007; Chen, et al., 2014; Fan, et al., 2012; Foley & Pollard, 2000; French, 1979; Gang, et al., 2014; Gao, et al., 2013; Han, et al., 2008; Herrmann, Anyamba, & Tucker, 2005; Horion, Cornet, Erpicum, & Tychon, 2013; Intergovernmental Panel on Climate Change, 2014; Li, 1997; Lieth, 1975; Lieth & Box, 1972; Liu & Zha, 2004; Lu, Batistella, Mausel, & Moran, 2007; Ma, Zhou, & Pei, 2012; Mu, et al., 2013; Mu, et al., 2013; O'Mara, 2012).

$$\boldsymbol{Humidity\ Index\ (K)} = \frac{\boldsymbol{MAP}}{(\mathbf{0.1} \times \boldsymbol{\Sigma\Theta})} = \frac{\boldsymbol{MAP}}{(\mathbf{0.1} \times \boldsymbol{GDD0})} \qquad \textbf{Equation 1}$$

Where:

- MAP is the mean annual precipitation (mm);
- GDD0 is Growing Degree-Days above 0℃, (i.e., mean annual accumulative temperature above 0℃)
- 0.1 is a justified coefficient of the model.

Based on decades of studies, 7 thermal zones and 6 humidity zones (Table 1, 2, 3) have been identified and used to differentiate vegetation classes. The CSCS recognizes 42 vegetation classes (Figure 2, Table 2,3).

2.2. Grassland productivity estimation

a. Grassland net primary production(NPP) estimates

Using the MODIS NDVI data and CASA (Carnegie-Ames-Stanford Approach) model and LPA model designed by ourselves, we calculate natural vegetation NPP in China from 2001 to 2010, and analyse its spatio-temporal dynamic and driving factors. Moreover, we will explore the relative roles of climate change and human activities on vegetation restoration or degradation. Furthermore, we calculate the global terrestrial vegetation NPP at different spatio-temporal scales using Zhou Guangsheng model.

Table 1 Classification of 7 thermal zones based on GDD0

Thermal grades	Growing degree-days on 0℃ base （GDD0）	Corresponding thermal zone
Frigid	＜1300	Alpine / frigid zone
Cold temperate	1300-2300	Cold temperate zone
Cool temperate	2300-3700	Cool temperate zone
Warm temperate	3700-5300	Warm temperate zone
Warm	5300-6200	Temperate subtropics
Subtropical	6200-8000	Equatorial subtropics
Tropical	＞8000	Tropics

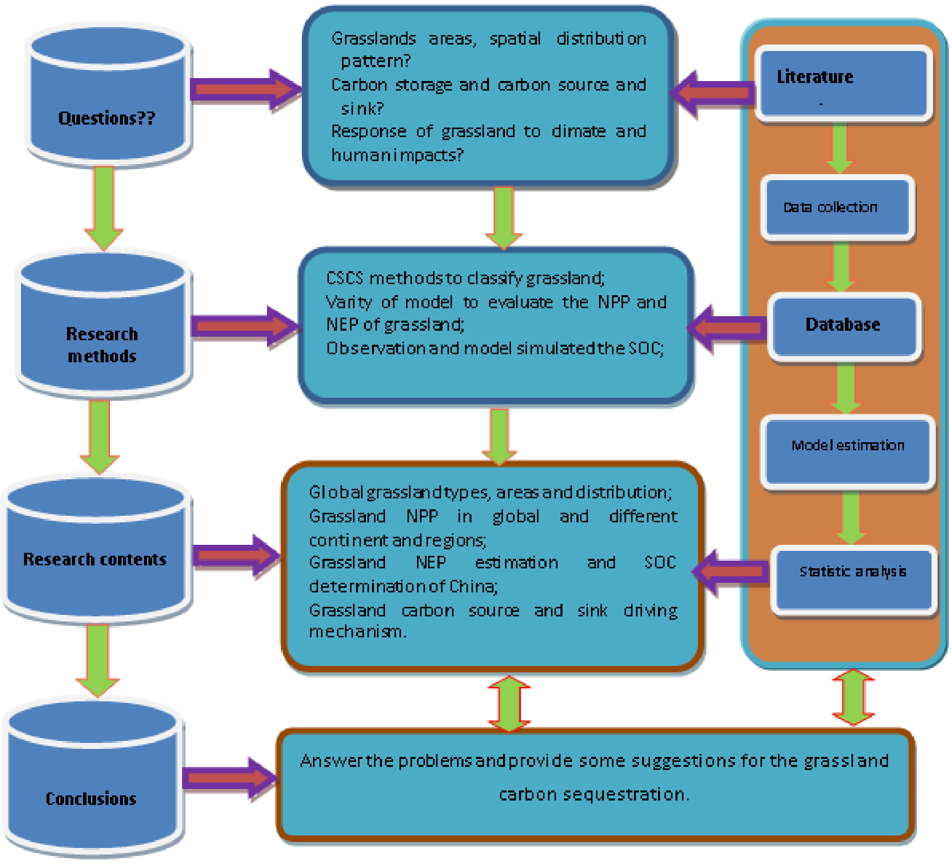

Figure 2 Global grassland carbon source and sink estimation technical route

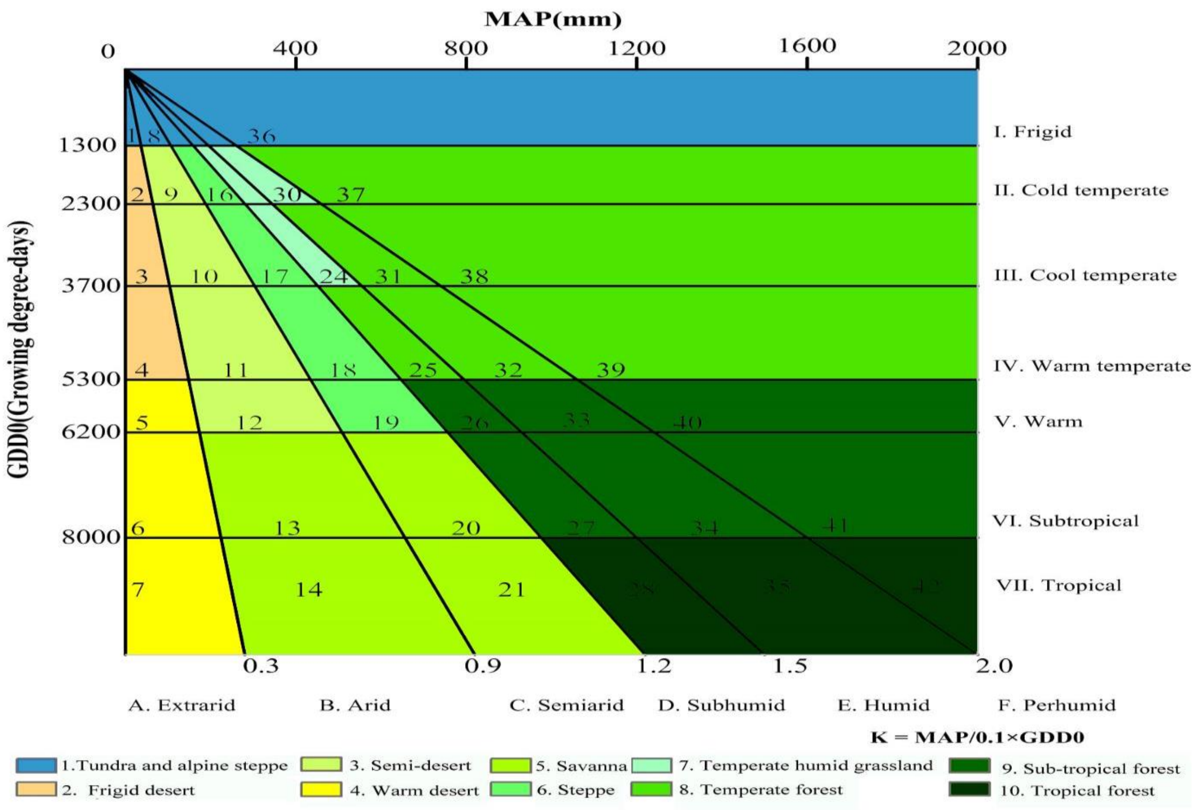

Figure 3 Index chart for determining PNV class and broad category in the CSCS model (42 classes and 10 broad categories) (Li, 1997)

Table 2 The classification of 6 humidity level based on K

Humidity degree	K-value	Corresponding natural landscape
Extrarid	＜0.3	Desert
Arid	0.3-0.9	Semi desert (desert steppe, steppe desert)
Semiarid	0.9-1.2	Typical steppe, xerophytic forest, savanna
Subhumid	1.2-1.5	Forest, forest steppe, meadow steppe, savannah, meadow
Humid	1.5-2.0	Forest, tundra, meadow
Perhumid	＞2.0	Forest, tundra, meadow

Table 3 The correspondence relation between 10 broad CSCS PNV categories and 42 classes

Name of broad category	Name of class
Tundra & alpine steppe	Frigid-extrarid frigid desert & alpine desert, Frigid-arid frigid zonal semi desert, alpine semi desert, Frigid-semiarid dry tundra, alpine steppe, Frigid-subhumid moist tundra, alpine meadow steppe, Frigid-humid tundra, alpine meadow, Frigid perhumid rain tundra, alpine meadow
Frigid desert	Cold temperate-extrarid montane desert, Cool temperate-extrarid temperate zonal desert, Warm temperate-extrarid warm temperate zonal desert
Semi-desert	Cold temperate-arid montane semi desert, Cool temperate-arid temperate zonal semi desert, Warm temperate-arid warm temperate zonal semi desert, Warm-arid warm subtropical semi desert
Warm desert	Warm-extrarid subtropical desert, Subtropical-extrarid subtropical desert, Tropical extrarid tropical desert
Savanna	Subtropical arid subtropical desert brush, Tropical arid tropical desert brush, Subtropical-semiarid subtropical brush steppe, Tropical-semiarid savanna, Tropical subhumid tropical xerophytic forest
Steppe	Cold temperate-semiarid montane steppe, Cool temperate-semiarid temperate typical steppe, Warm temperate-semiarid warm temperate typical steppe, Warm-semiarid subtropical grasses-fruticous steppe
Temperate humid grassland	Cold temperate-humid montane meadow, Cool temperate-subhumid meadow steppe, Cold temperate-humid montane meadow, Cool temperate-humid forest steppe, deciduous broad leaved forest
Forest, including temperate forest, sub-tropical forest and tropical forest	Warm temperate-subhumid forest steppe, Warm temperate-humid deciduous broad leaved forest, Warm temperate perhumid deciduous broad leaved forest, Cool temperate perhumid mixed coniferous broad leaved forest, Cold temperate perhumid taiga forest, Warm-subhumid deciduous broad leaved forest, Subtropical-subhumid sclerophyllous forest, Warm-humid evergreen-deciduous broad leaved forest, Subtropical-humid evergreen broad leaved forest, Warm-perhumid deciduous-evergreen broad leaved forest, Subtropical perhumid evergreen broad leaved forest, Tropical-humid seasonal rain forest, Tropical perhumid rain forest

Based on global climate dataset derived from CRU-TS2.1 (Climate Research Unit), which consists of multi-variate mean monthly climatology records at 0.5° x 0.5° resolution for global land areas (excluding Antarctica) for the period 1911-2011, we classify the global natural vegetation and analyse its NPP of different vegetation types at different spatio-temporal scales (Rojstaczer, Sterling, & Moore, 2001; Scurlock & Hall, 1998; Sekiyama, Takeuchi, & Shimada, 2014; Wang, Sun, Han, & Yan, 2012; Wessels, et al., 2007; Xu D. Y., Kang, Liu, Zhuang, & Pan, 2009; Xu D. , Kang, Liu, Zhuang, & Pan, 2010; Xu, et al., 2011; Yeh, 2005; Ykhanbai, Bulgan, Beket, Vernooy, & Graham, 2015).

CASA model

NPP was calculated using the CASA model in Figure 4, and it is based on the product of Absorbed Photo synthetically Active Radiation (APAR) and light-use efficiency (ε). The basic principle of the model can be described by the following formula:

$$\boldsymbol{NPP\ (x,t) = APAR\ (x,t) \times\ \varepsilon\ (x,t)} \qquad \textbf{Equation 2}$$

Where: *x* is location (the pixel number) and *t* is time. APAR represents the canopy-absorbed incident solar radiation integrated over a given time period (MJ/m2) and ε *(x, t)* represents the actual light use efficiency (g C/MJ) of pixel *x* in *t* time.

Estimation of APAR:

$$\boldsymbol{APAR\ (x,t) = SOL\ (x,t) \times FPAR\ (x,t) \times 0.5}$$

Equation 3

Where *SOL (x, t)* is the total solar radiation (MJ/m2) of pixel *x* in *t* time. *FPAR (x, t)* is the fraction of PAR absorbed by vegetation canopy, 0.5 stands for the fraction used for vegetation.

Estimation of ε:

$$\varepsilon(x,t) = T_{\varepsilon 1}(x,t) \times T_{\varepsilon 2}(x,t) \times W_{\varepsilon}(x,t) \times \varepsilon_{\max} \qquad \textbf{Equation 4}$$

Where: $T_{\varepsilon 1}(x,t)$ and $T_{\varepsilon 2}(x,t)$ are temperature stress coefficients which reflect the reduction of light-use efficiency caused by temperature factor; $W_{\varepsilon}(x,t)$ is the moisture stress coefficient; ε_{max} is the maximum light-use efficiency under ideal conditions.

Zhou Guangsheng model

This model estimated NPP based on the water-balance and heat-balance equations. The model was expressed as follows:

$$\mathrm{NPP} = \mathrm{RDI}^2 \times \frac{r\left(1 + RDI + RDI^2\right)}{\left(1 + RDI\right)\left(1 + RDI^2\right)} \times e^{-\sqrt{9.87+6.25RDI}}$$ **Equation 5**

$$RDI = \left(0.629 + 0.237 \times PER - 0.00313 \times PER^2\right)^2$$ **Equation 6**

$$PER = 58.931 \times BT/r$$ **Equation 7**

Where: *PER* is the potential evaporation; *BT* is the monthly mean biomass temperature for temperature ranging between 0 and 30℃; and *r* is the annual precipitation (mm). This model is climate productivity model only based on the climate data such as temperature and precipitation.

Thornthwaite Memorial Model：

The Thornthwaite Memorial model was established based on the data used in the Miami model, but was modified to include Thornthwaite's potential evaporation model. The model was expressed as follows:

$$NPP = 3000\left[1 - e^{-0.0009695(v-20)}\right]$$ **Equation 8**

$$V = \frac{1.05r}{\sqrt{1 + \left(1 + 1.05r/L\right)^2}}$$ **Equation 9**

$$L = 3000 + 25t + 0.05t^3$$ **Equation 10**

Where: *v* is the annual average actual evapotranspiration (mm), L is annual average evapotranspiration (mm), *r* is annual precipitation (mm), *t* is the annual average temperature (℃).

b. Grassland net ecosystem production(NEP) estimation

Carbon flux is important to carbon storage and carbon cycle. Here we calculate NEP through model estimation, such as BEPS model and Biome-BGC model. The estimation process based on BEPS model is as follows in Figure 5:

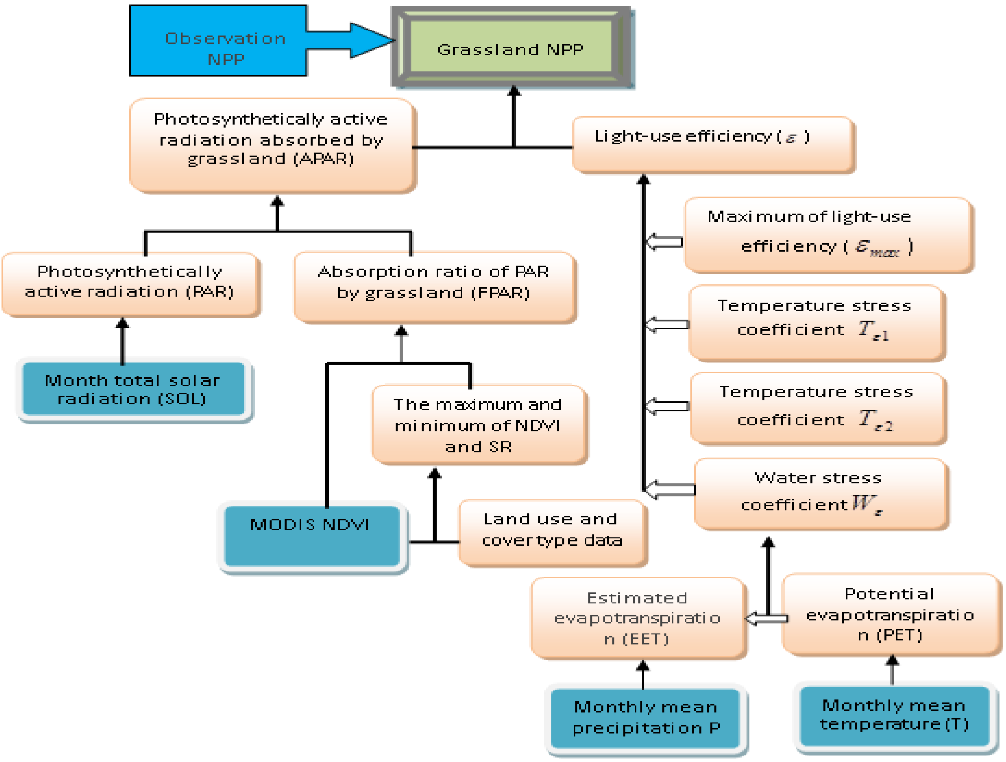

Figure 4 CASA model estimation of NPP

c. Grassland soil organic carbon estimation

We explore the mechanism and process of carbon (especially soil carbon carbon) cycle at regional and global scale using field observation data, and build proper terrestrial vegetation biological process model and remote sensing retrieval.

Soil is the largest organic carbon reservoir in terrestrial biosphere, about two times larger than that of vegetation or atmosphere, and thus plays a crucial role in the terrestrial carbon cycle. Although a minor change of SOC storage could result in a significant alteration of atmosphere CO_2 concentration. Therefore, accurate estimation of SOC storage and its distribution is critical for predicting feedbacks of soil C to global environmental change. Additionally, grassland as the most important ecosystem in the world, plays an important role in the global terrestrial C cycle due to their large area and high proportion of belowground C stock. They likely contribute as much as 20% of the total terrestrial production and provide an annual sink of 0.5 P g C. A quantitative assessment of grassland carbon storage and its temporal dynamics in grassland ecosystems is thus the basis to accurately evaluate C sinks or sources in global terrestrial C cycling. Moreover, identifying the effects of climate change on biomass C dynamics in grassland ecosystems is critical to predicting the response of grassland ecosystems to future climate change. However, large uncertainties still exist in estimates of grassland carbon storage and its response to climate change. In addition, previous estimates have been mainly based on field surveys from the 1960s to 1980s, which limits our understanding of the current carbon storage in grassland ecosystem.

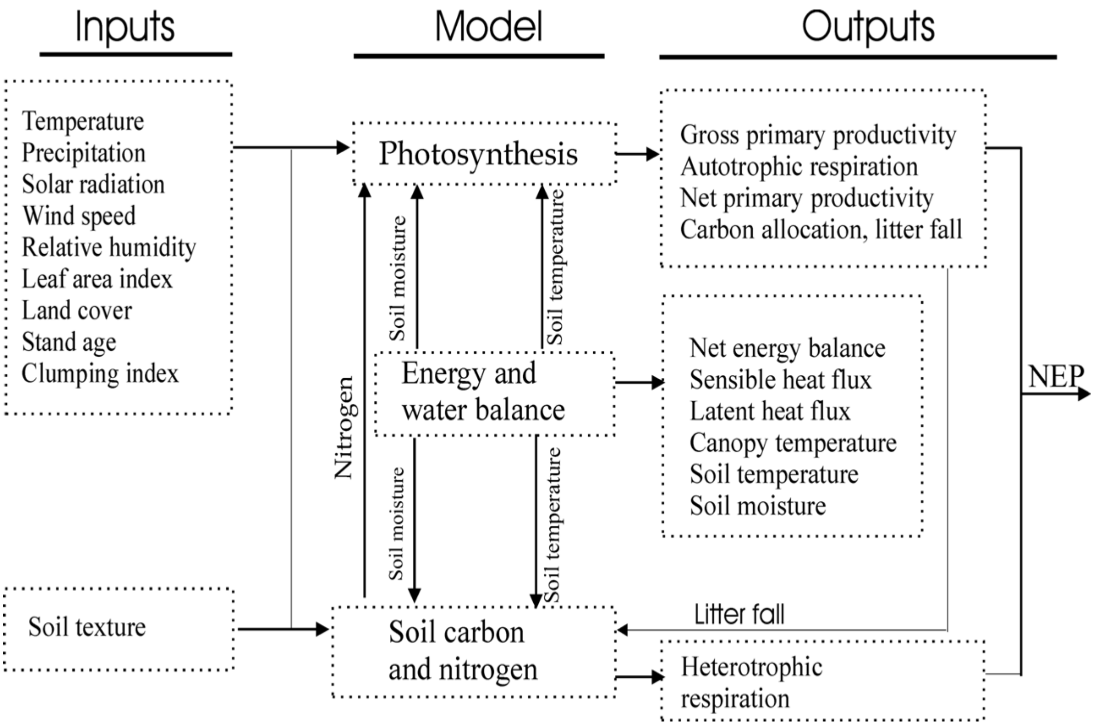

Figure 5 BEPS model estimation of NEP

1) Remote sensing retrieval SOC

Based on the above conclusions, firstly, we will make a large scale field survey in China and reference previous researches SOC density database. Then we established the site-level relationship between SOC density and remote sensing dataset such as NDVI or EVI, and then to estimate the SOC in a large scale through remote sensing retrieval. Moreover, we analysed the spatial-temporal change of SOC of China from the 1980s to 2010s, and explore the response of carbon storage to environmental changes.

2) Century model simulate the SOC:

Soil Organic Carbon can be also estimated by the Century model, the model calculation process show in the following diagram 6-7.

3) Hyperspectral detection SOC method:

At the same time, soil organic carbon (SOC) can be predicted by hyperspectral retrieval method.

— Soil samples: Soil samples plots were set in the typical grassland. And soil sample were collected and the SOC were measured in laboratory.

— Hyperspectral detection: The reflectance of the soil samples was measured in the field with the FieldSpec TM Pro JR portable spectrometer. The FieldSpec TM Pro JR spectrometer has a light source and measurements are made using the contact probe. It offers a full spectral range (350–2500 nm) and rapid data collection (10 scans per second). A white spectral on panel (5×5 cm) provided the absolute reflectance factor for field measurements. The surface scanned was a core of 10 cm and 10 scans were made per sample. The spectral on panel was systematically measured before each sample measurement, using 50 replicates. A spectrum reflection curve was recorded by the ViewSpec Pro 4.02 spectrum processing software.

— Prediction of SOC: Partial least-squares regression (PLSR) with leave one-out cross validation was used for SOC predictions using both the field spectra and the Hyperion remotely-sensed satellite data in SAS software. The root mean squared error (RMSE), coefficient of determination (R2) and ratio of performance to deviation (RPD) were used to evaluate the performance of SOC prediction models.

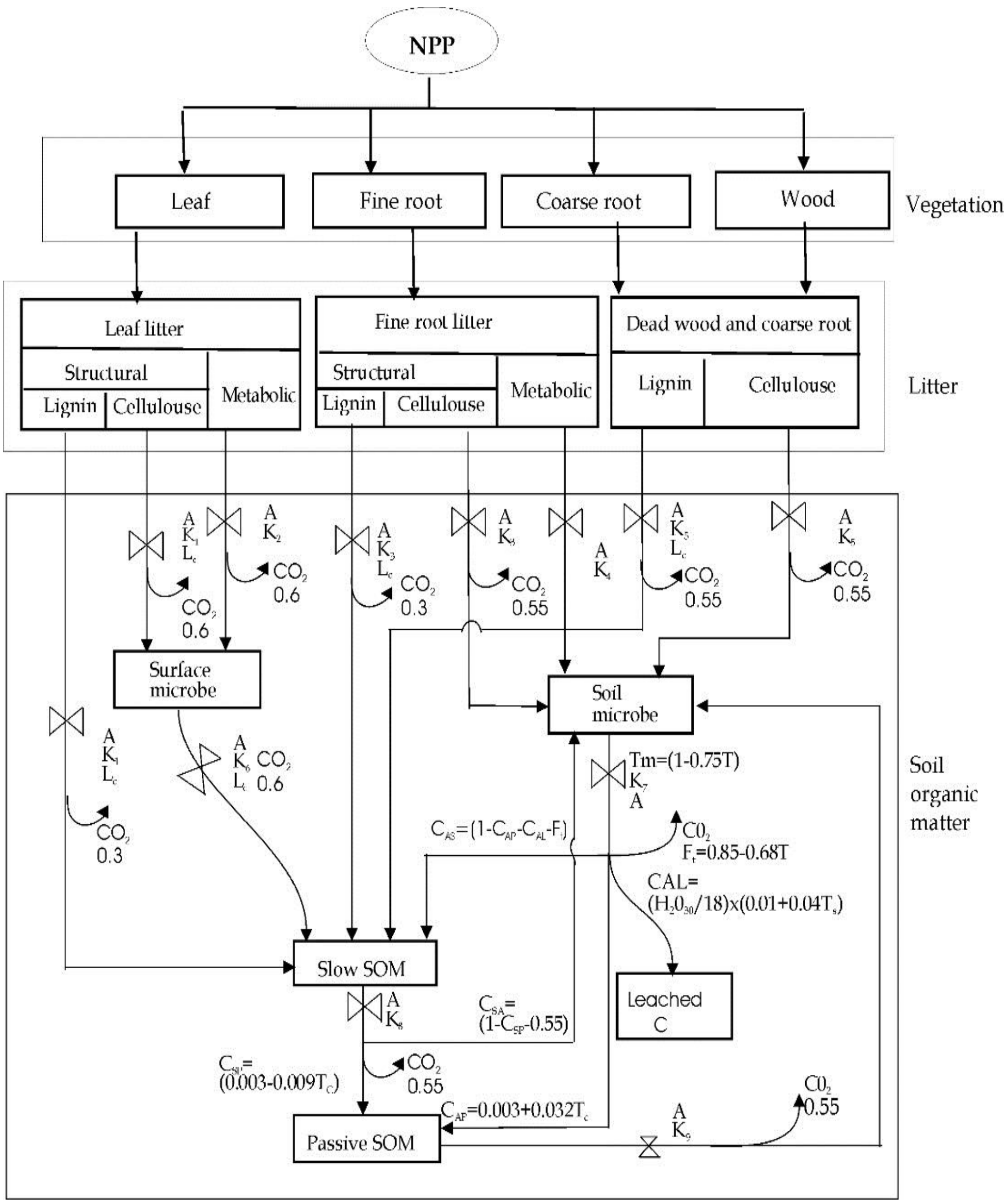

Figure 6 Estimation SOC based on Century model

— Global potential natural vegetation (PNV) was classified using CSCS method based on CRU's climate data from 1911 to 2000. The PNV in continents, such as Asia, Europe, Africa, America and Oceania, was simulated and compared. The NPP changing trend under different temporal-spatial conditions was also analysed. Meanwhile, we predict the effects of the future extreme climate change and land use change on carbon cycle and carbon storage and their changing trend using the CA model built by ourselves.

— The simulated results of different models, including CASA model, Century model, BEPS model, LPA model and Projection Pursuit Regression model were compared through the filed observation data, remote sensing data and the atmospheric reflection data. Through the validation of the simulation results that derived from the above different models, the global grassland classification, spatial distribution, NPP, biomass, soil organic carbon and the total carbon storage of different continents are calculated; the changing trend of the above parameters in respond to climate change are also analysed (Rojstaczer, Sterling, & Moore, 2001; Scurlock & Hall, 1998; Sekiyama, Takeuchi, & Shimada, 2014; Wang, Sun, Han, & Yan, 2012; Wessels, et al., 2007; Xu D. Y., Kang, Liu, Zhuang, & Pan, 2009; Xu D. , Kang, Liu, Zhuang, & Pan, 2010; Xu, et al., 2011; Yeh, 2005; Ykhanbai, Bulgan, Beket, Vernooy, & Graham, 2015; Yong-Zhong, Yu-Lin, Jian-Yuan, & Wen-Zhi, 2005; Zhang, Wang, Li, & Hua, 2011; Zheng, Xie, Robert, Jiang, & Shimizu, 2015; Zhou W. , et al., 2015; Zhou W. , et al., 2014) (see Figure 6-7).

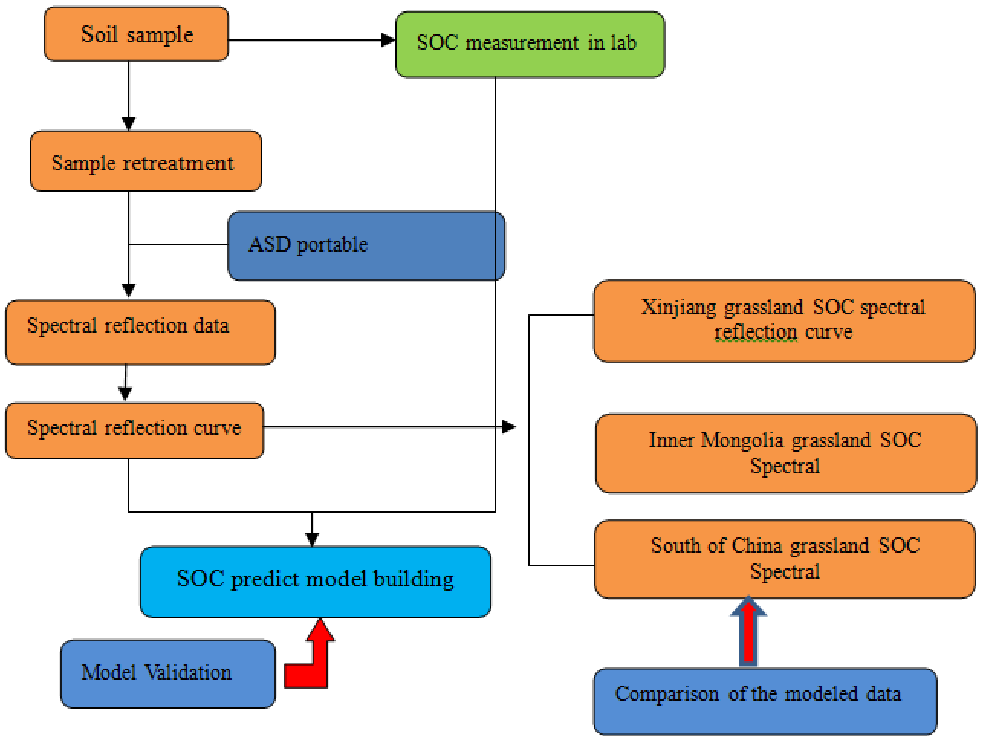

Figure 7 Hyperspectral detection SOC technical route

4) Grassland carbon storage estimation and evolution trends evaluation in Figure 8-10.

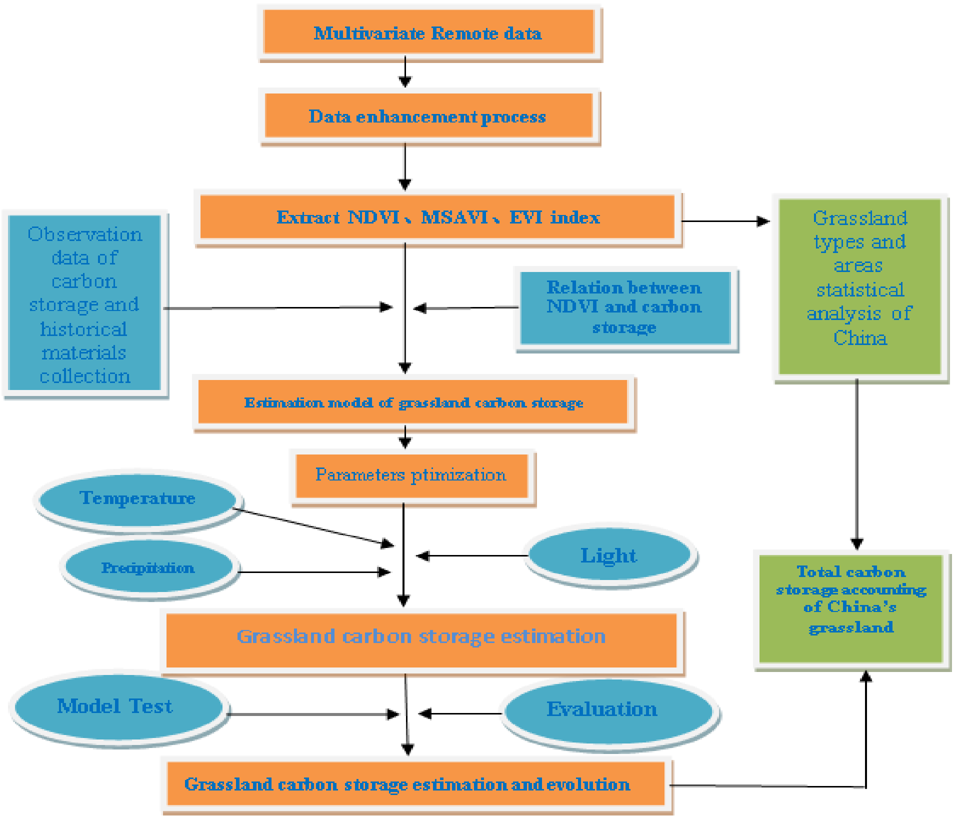

Figure 8 Grassland carbon stocks estimation and evolution analysis

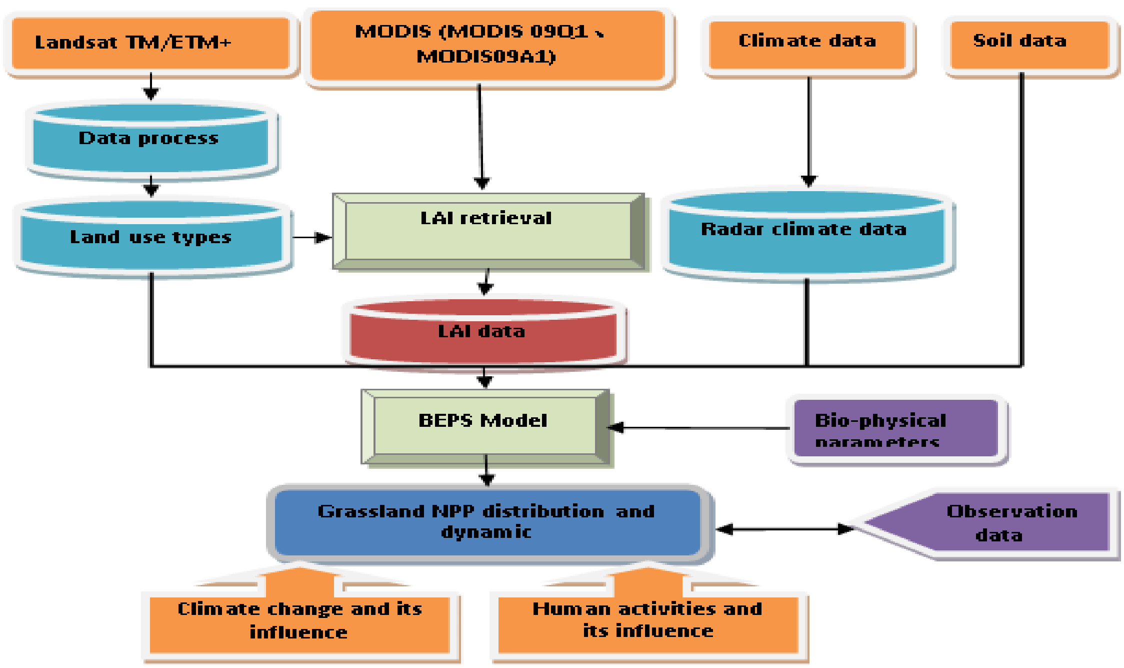

Figure 9 Estimation of grassland NPP based on BEPS Model

Figure 10 Grassland carbon storage dynamic and driving mechanism analysis

3. Results & Discussions

3.1. The NPP of grasslands in China, Mongolia, Pakistan and Uzbekistan during 2000-2013

The spatial distribution of grassland NPP was represented in the four countries from 2000 to 2013 (Figure 11). The distribution of Chinese grassland NPP decrease trend from the southeast of China to the northwest. The highest value of grassland NPP was located in the Yunnan-Guizhou Plateau. In Mongolia, the changing trend of grassland NPP was decreased from north to south and the value of Hovsgol grassland NPP was the highest in Mongolia. In Pakistan, the grassland NPP was higher in the Islamabad than other regions. The spatial distribution of grassland NPP was not occur evenly, and the trend was increase from the south to north. By compare the grassland NPP in these four countries, the value of grassland NPP was highest in China, followed by the Mongolia, Pakistan and Uzbekistan. The average of grassland NPP during the period of 2000-2013 was 1112.827 Tg C in China, 161.011 Tg C in Mongolia, 26.66 Tg C in Pakistan and 16.39 Tg C in Uzbekistan (table 4) (Yang, 2017).

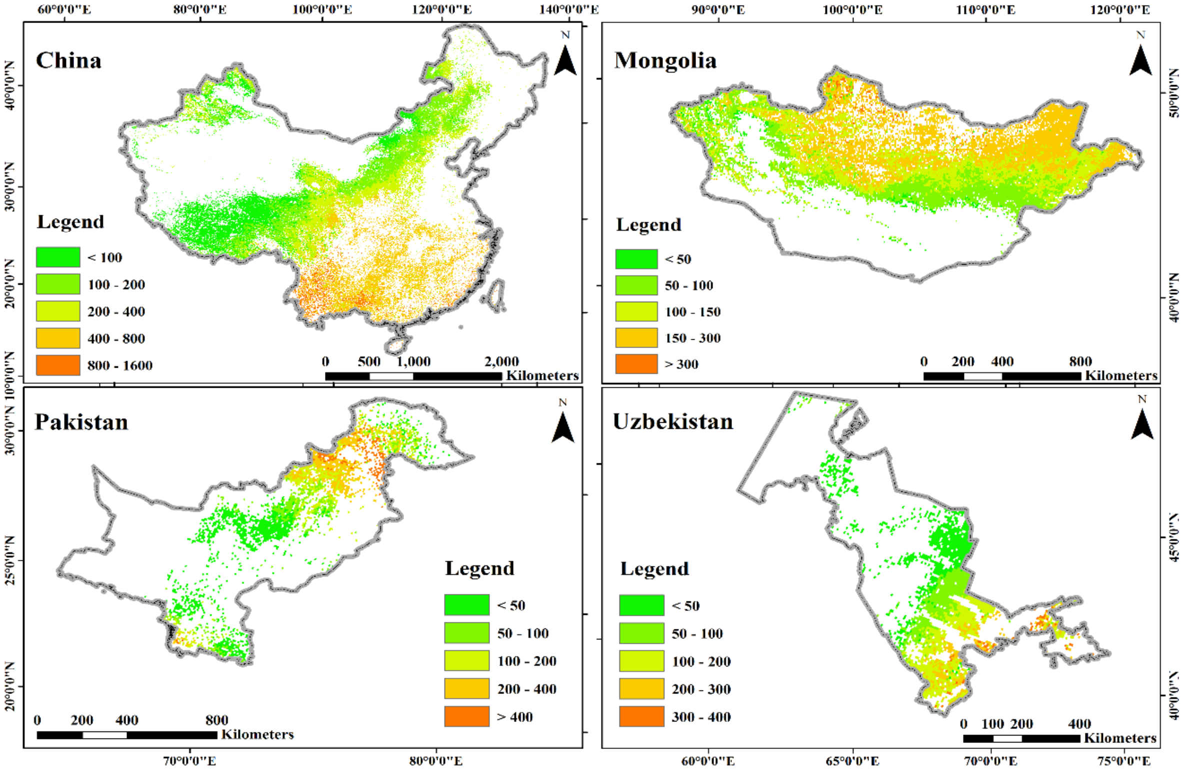

Figure 11 The spatial distribution of grassland NPP in these four countries (g C/m2/year) (Yang, 2017)

Table 4 The NPP of grasslands in China, Mongolia, Pakistan and Uzbekistan during 2000-2013 (Unit: Tg C**)** (Yang, 2017)

Year	China	Mongolia	Pakistan	Uzbekistan
2000	1009.22	159.24	23.24	13.16
2001	1016.67	151.42	24.26	13.23
2002	1141.95	156.29	22.78	18.50
2003	1136.14	172.32	27.62	20.78
2004	1137.03	146.13	25.14	20.28
2005	1091.19	156.58	28.14	17.96
2006	1144.32	153.92	26.85	15.13
2007	1121.84	130.39	29.97	15.74
2008	1126.63	157.75	27.32	11.98
2009	1125.91	153.82	22.56	22.08
2010	1093.87	155.67	28.55	17.00
2011	1092.66	176.70	29.48	11.01
2012	1139.97	194.79	26.60	15.32
2013	1202.17	189.14	30.67	17.37

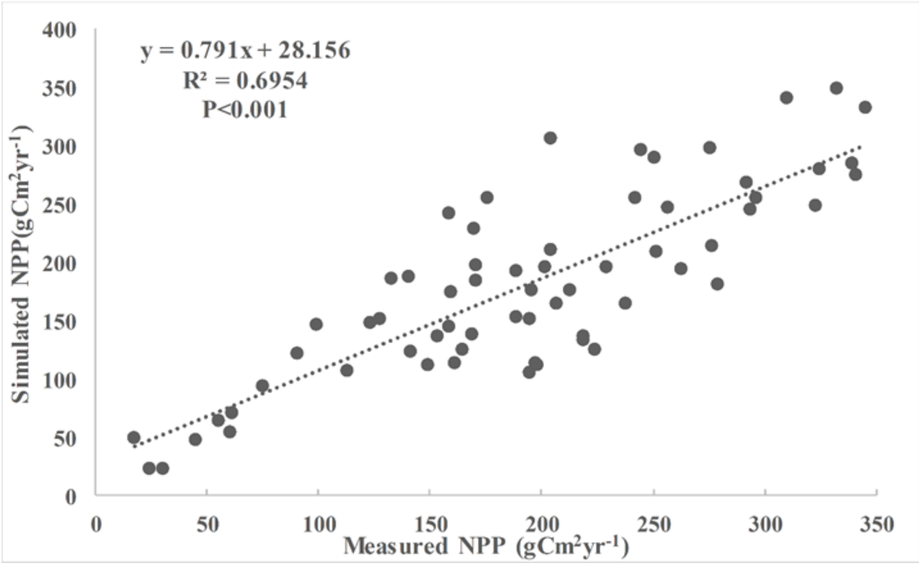

Figure 12 The validation of the grassland NPP simulated by CASA model (g C/m^2/year) (Yang, 2017)

The NPP determined from the field sampling was compared with the simulated values to verify the estimation accuracy of the CASA model. The correlation between the observed NPP and the estimated NPP (R^2 =0.6954, P < 0.001) indicated that the CASA model exhibited a satisfactory estimation accuracy in estimating NPP (Yang, 2017). The simulated NPP was slightly larger than the actual field data. However, these differences did not alter the results of the model.

Calculated by the least squares method, simple linear regression was employed to analyze the inter-annual variation of grassland NPP dynamics at a global scale from 2000 to 2013. The slope of the trend line in the multiyear regression equation for a single pixel represents the inter-annual variation rate, which is solved by the ordinary least-squares method. We found that the interannual variability of China grass growth trends, the extent of growth is less (R^2=0.3277), and interannual variability of Mongolia grassland is the trend of growth, and with the less amplitude (R^2=0.2656). Through to the Pakistan grass observation found that the interannual NPP grow larger (R^2=0.366). By contrast, the grassland NPP decline slightly (R^2=0.0044) in the Uzbekistan (0).

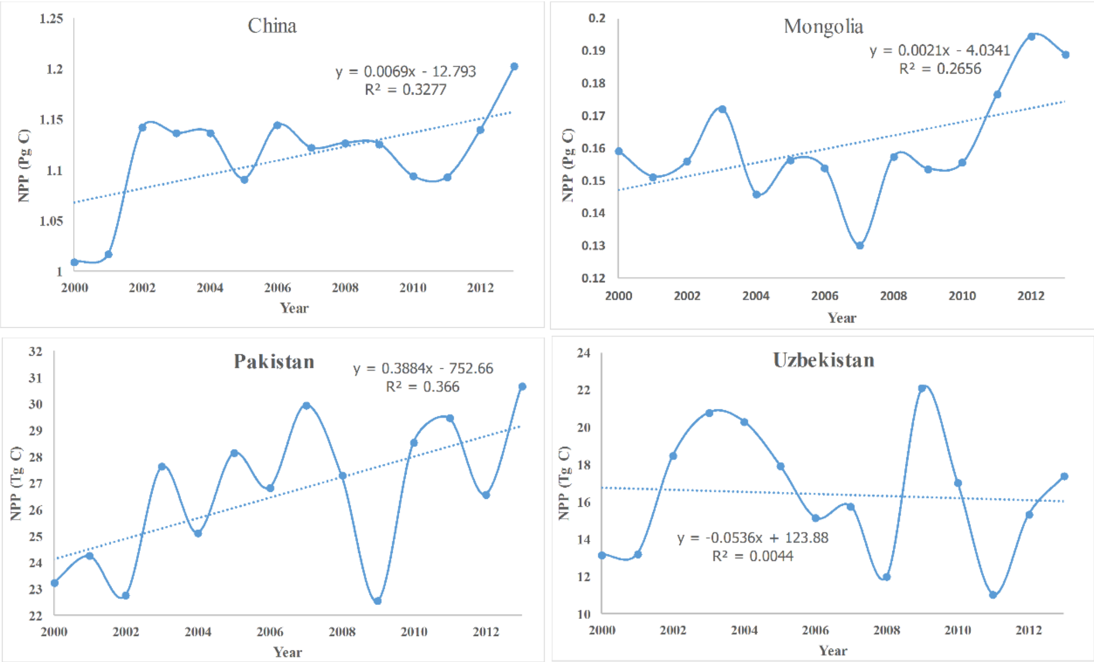

Figure 13 The inter-annual variation of grassland NPP in these four countries (Pg C in China and Mongolia; Tg C in Pakistan and Uzbekistan) (Yang, 2017)

3.2. The carbon storage in China, Mongolia, Pakistan and Uzbekistan based on CASA model and climate controls in these four countries

3.2.1. Grassland ecosystem storage and its spatial patterns

The CASA model estimated that the biomass carbon storage was 1.47 Pg C, 0.44 Pg C, 0.03 Pg C, 0.03 Pg C in China, Mongolia, Pakistan and Uzbekistan, respectively. By contrast, the soil carbon storage was 29.25 Pg C, 13.86 Pg C, 0.46 Pg C, 0.29 Pg C in these four regions (table 5). The grassland carbon storage contained the biomass carbon storage and soil carbon storage. Among these four countries, the soil carbon storage accounted for most of the total carbon storage, and the proportions were all over 90%. As China had the largest areas of grassland, it had the most grassland carbon storage among the four countries. Mongolia had the second largest carbon storage. And, followed by Pakistan and Uzbekistan.

It should be noted that our model results were close to the estimates made by Ma et al. (2016). For instance, it was estimated that the biomass carbon storage was 1.61 Pg C and SOC storage was 29.37 Pg C using six methods (three spatial interpolation methods and three grassland classification methods) to estimate carbon storage of Chinese grasslands based on published data. Fang, et al. (2010)'s estimation of biomass carbon and SOC storage also agreed with the results of our study.

Table 5 The carbon storage of grasslands in China, Mongolia, Pakistan and Uzbekistan (Unit: Pg C)

	China	Mongolia	Pakistan	Uzbekistan
Biomass carbon storage	**1.47**	**0.44**	**0.03**	**0.03**
Soil carbon storage	**29.25**	**13.86**	**0.46**	**0.29**
Grassland carbon storage	**30.72**	**14.30**	**0.49**	**0.32**
Study result of Ma (2016)	**30.98**	**-**	**-**	**-**
Study result of Fang (2010)	**29.10**	**-**	**-**	**-**

3.2.2. Spatial distribution of grassland ecosystems carbon storage in the four regions

The distribution of biomass carbon storage was discovered in Figure 14. In general, the biomass carbon density of grassland decreased from southeastern China toward the northwest. The mean biomass carbon density was 0.41 kg C m^{-2} and the range of carbon density was 0.1-1.33 kg C m^{-2}. The higher mean carbon density of grassland was found in the southeast of Qinghai province, West Sichuan Plateau and Gannan Plateau, where the biomass carbon storage per unit area was above 0.7 kg C m^{-2}, and the largest value was 1.33 kg C m^{-2}. In Mongolia, the higher carbon storage was distributed in the north part, the carbon density decreased from north to south. In Pakistan, the higher carbon density was found around the Islamabad and the largest carbon density was 1.23 kg C m^{-2}. The carbon density of Uzbekistan was generally lower than the other three countries.

The results showed that the spatial pattern of soil carbon storage in China, Mongolia, Pakistan and Uzbekistan had obvious regional differences (Figure 15-16). According to the simulated results, the total SOC storage of Chinese grassland was 29.25 Pg C and the distribution of SOC storage in China showed an obvious zonal pattern. The lowest values (<5 kg C m^{-2}) appeared in dry regions near deserts, and the highest values (>25 kg C m^{-2}) were found in humid regions such as the parts of Hulunbeir Grassland, southeastern fringe of the Qinghai-Tibetan Plateau and Altay Prefecture of Xinjiang province. In Mongolia, the highest values (>25 kg C m^{-2}) were found in the north of Mongolia, and most in the Huvsgel province. The situation of the distribution of soil carbon storage in Pakistan and Uzbekistan were similar with the distribution of biomass carbon storage and the Uzbekistan had the lowest carbon density among these four regions.

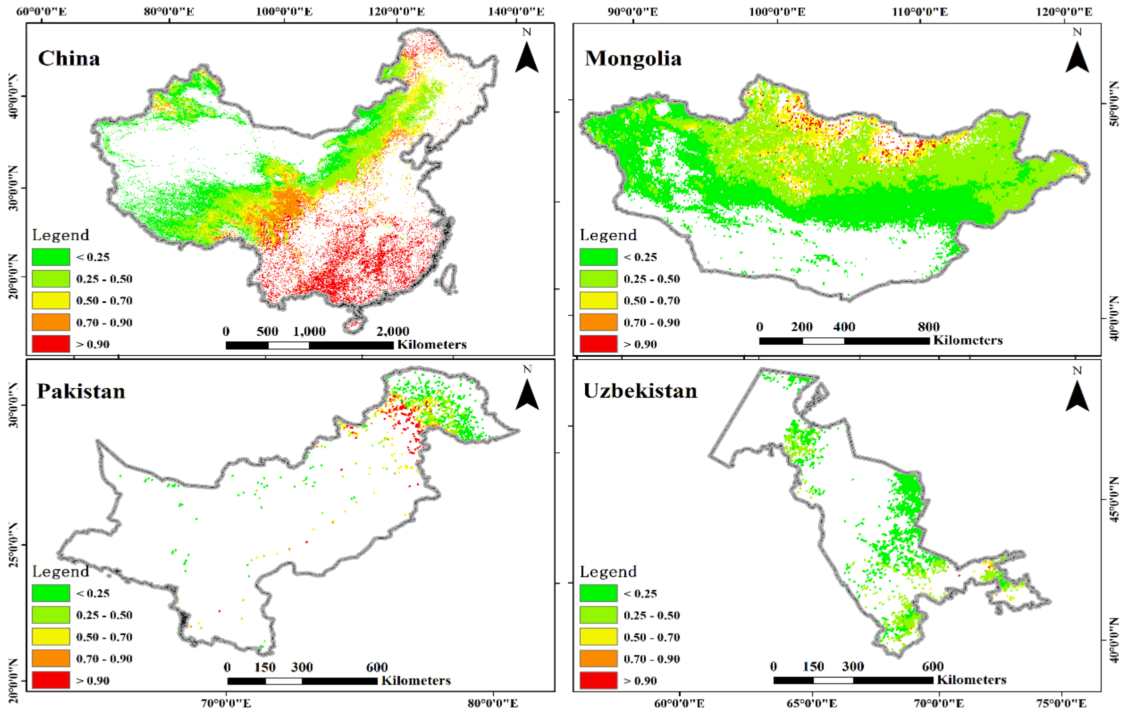

Figure 14 The spatial distribution of biomass carbon storage in these four countries (kg C m^{-2}) (Yang, 2017)

This study did not consider the human activities and land use change on the influence of grassland ecological system, so the carbon stock changes mainly affected by climate change. A lot of research has shown that the grassland ecosystem carbon cycle is influenced by climate factors such as rainfall and temperature which is significant affected the carbon cycle. The climate variation influenced terrestrial vegetation mainly through precipitation and temperature changes, which further regulated soil respiration, photosynthesis, and growing status and distribution. As the rainfall was good for the growth of vegetation, especially in dry land, the grassland carbon storage was higher in the areas with high rainfall. And the low temperature in the meadows of these four regions, hence soil organic carbon decomposes slowly, causing the soil organic carbon density to be high. However, in some areas the carbon storage is affected by the humid climate, therfore the biomass carbon density is higher. By contrast, the warm climate stimulates soil organic carbon decomposition and conduces the lower soil carbon density.

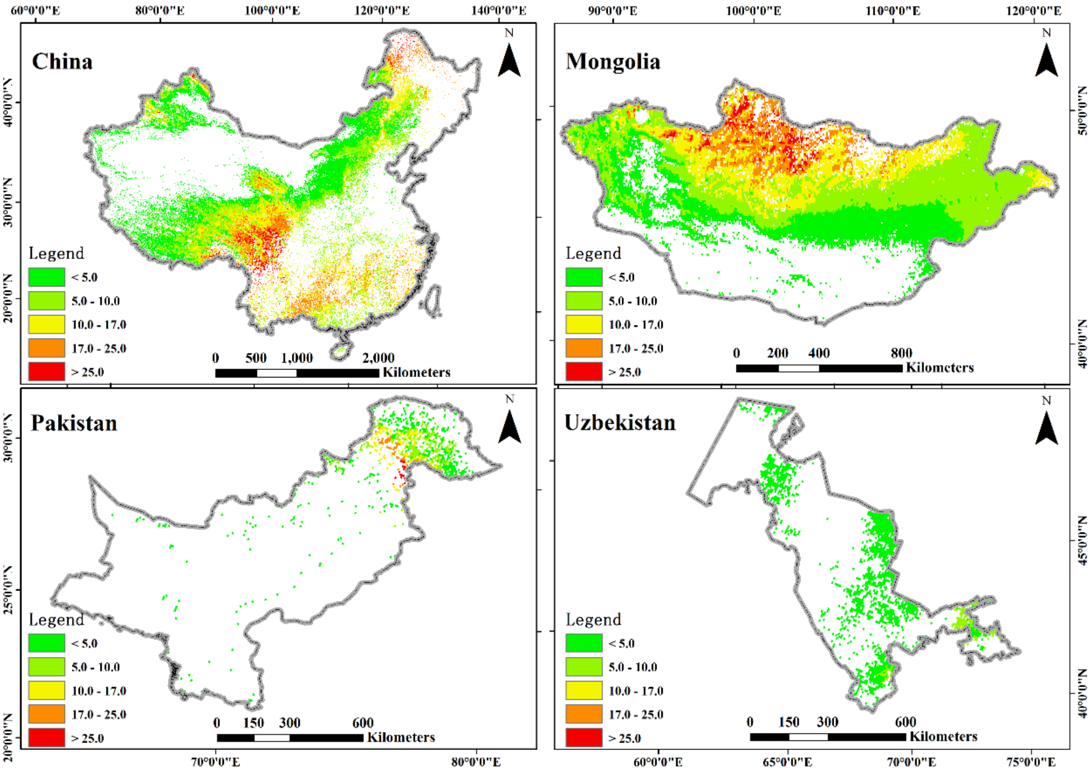

Figure 15 The spatial distribution of SOC storage in these four countries (kg C m^{-2}) (Yang, 2017)

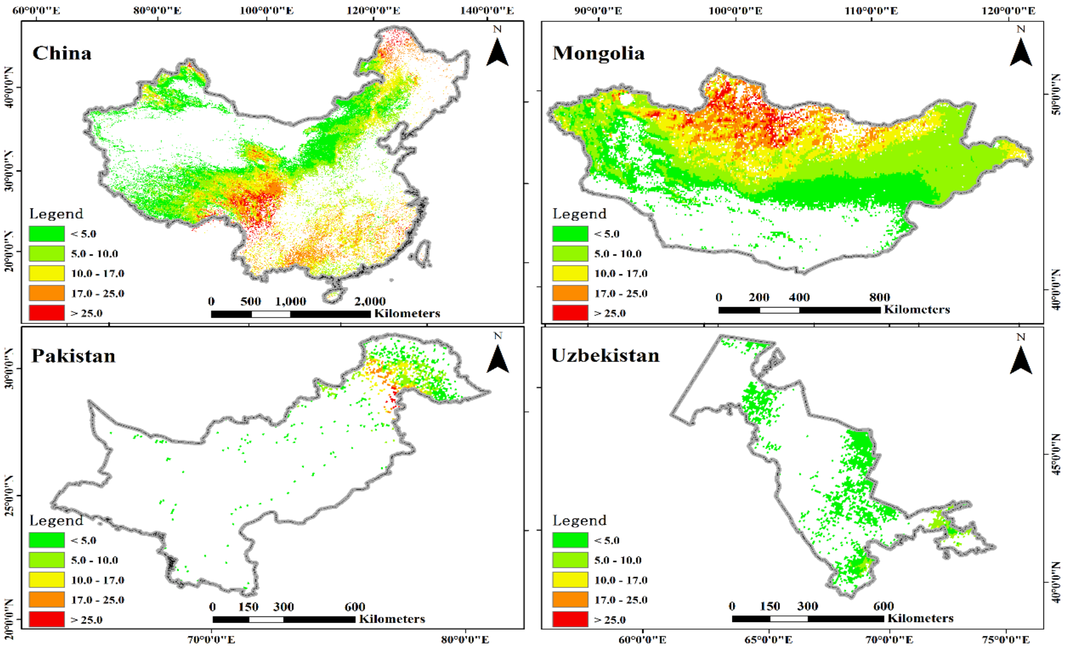

Figure 16 The spatial distribution of whole grassland carbon storage (kg C m^{-2}) (Yang, 2017)

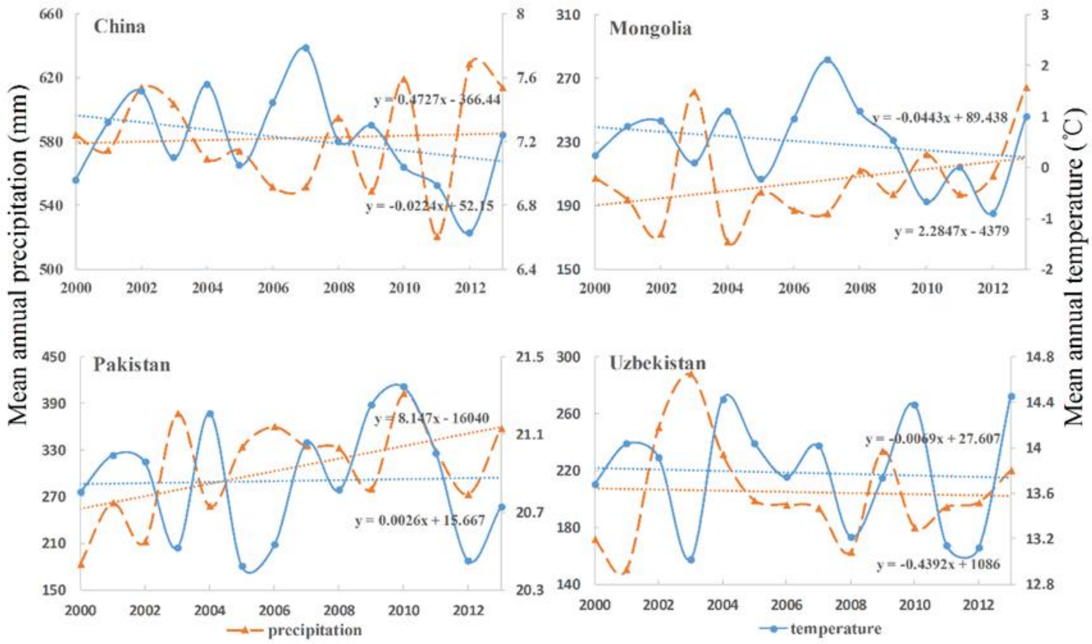

Figure 17 The changing trends of climate factors in the four countries from 2000 to 2013 (Yang, 2017)

Precipitation change by changing the water by vegetation growth and soil microbial activity, as well as the soil moisture content, to influence the litter carbon to the soil type and soil respiration rate, and thus affect the grassland ecosystem carbon library. And the temperature change is a major role in plant photosynthetic rate, plant root respiration and soil microbial activity, thereby affect the ecological system input and output of carbon library. Therefore, the change of the grassland ecosystem carbon depends on the balance between input and output.

3.3. The grassland net ecosystem productivity (NEP) of these four countries based on CASA model

3.3.1. The spatial distribution of grassland NEP in these four countries

The distribution of grassland NEP in China was presented in Figure 18. We can see from the fig18, the general distribution characteristics of the grassland NEP higher from north to south, the central and northeast of China was low, the grassland NEP in Qinghai-Tibet Plateau was high. The carbon sources (NEP < 0) was mainly located in Sichuan Basin, northeast part of Inner Mongolia. The carbon sink (NEP > 0) was mainly distributed in the southeast of Tibetan. In Mongolia, the carbon sources (NEP < 0) was mainly located in the central and east of Mongolia. The carbon sink (NEP > 0) was mainly distributed in the Hovsgol. By contrast, the grassland is a weak carbon sinks in Pakistan. And the grassland in Uzbekistan was almost the carbon sinks. Through the table 6, we found that the annual average grassland NEP in China was 0.01448 Pg C/year, which showed the grassland ecosystem absorb carbon dioxide from the atmosphere. In Mongolia, the grassland annual average NEP was negative value (-0.00725 Pg C/year), which explained that the grassland ecosystem released the carbon dioxide into the atmosphere. In Pakistan, the grassland annual average NEP was negative value (-0.00037 Pg C/year). Both the grassland in Mongolia and Pakistan are weak carbon source, and the Pakistan was even weaker when compared with the grassland NEP in Mongolia. In Uzbekistan, the annual average grassland NEP was 0.00139 Pg C/year.

Table 6. The annual average NEP of grasslands in China, Mongolia, Pakistan and Uzbekistan **(Yang, 2017)**

	China	Mongolia	Pakistan	Uzbekistan
NEP (Pg C/year)	**0.01448**	**-0.00725**	**-0.00037**	**0.00139**

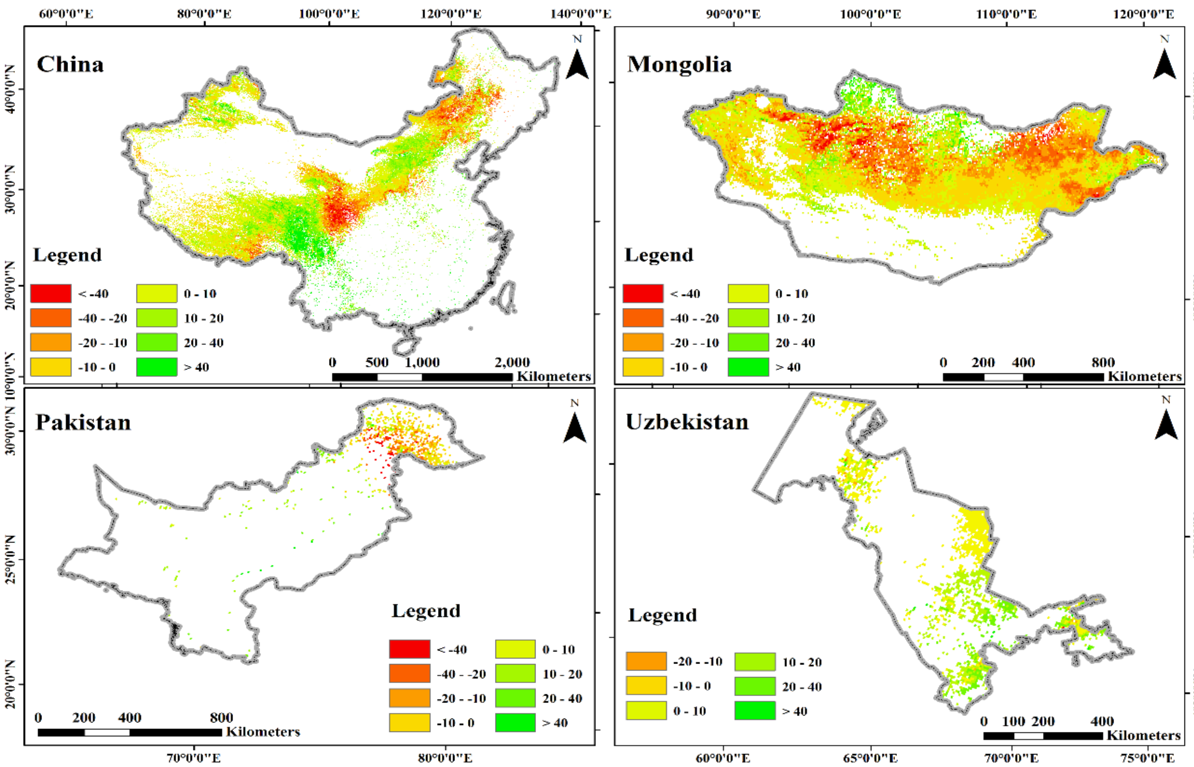

Figure 18 The spatial distribution of grassland NEP in these four countries (gC/m^2/year) (Yang, 2017)

3.3.2. The dynamic analysis of grassland NEP in these four countries

Figure 19 is obtained by least square fitting of the NEP trend chart. The dynamic of grassland NEP in these four countries is diverse from each other. In China, the grassland NEP decline was mainly located in Hulun buir grassland in the northeast of China. And grassland NEP in the central of Mongolia reduced significantly. By contrast, the grassland NEP fall mainly distributed around the Islamabad in Pakistan, and the reduction of grassland NEP in Uzbekistan is less, the lowest value is 0.98 g C/m^2/year.

Figure 20 for the variability of spatial distribution of annual precipitation, nationally, decadal carbon absorption increase/decrease area basically consistent with the increase or decrease in rainfall decadal area. This shows that in the national scale, the precipitation is the NEP spatial pattern of the main climate factor of change, but its role in different regions also have certain differences. The NEP in the north and inter-annual NPP, and the southern region is related to soil respiration. On the national scale, NPP and HR have better correlation with precipitation and temperature respectively, the NEP as their difference nature is affected by the common temperature and precipitation changes, just in different regions vary their degree of the impact of the NEP. The grassland NEP increases with the increase of atmospheric CO_2 concentration and precipitation, the grassland NEP decrease with temperature rising (Figure 20-21).

Need to point out that the difference in value as the NPP and soil respiration, the NEP the uncertainty of the estimating results is far greater than the NPP, and this is only driven by climate change a change in the pattern of regional carbon balance of payments may be an estimate. From the model itself, CASA model only considers the climate change and the CO: concentration increase, there is no consideration of land use/cover change, forest regeneration and pests, fire and other natural disturbances on terrestrial carbon balance, the influence of these have caused a lot of uncertainty for the results of the study, especially the land use/cover change is an important driving factor of carbon balance changes. In recent years, the land use and cover change on the influence of the carbon balance research more is to use based on the statistical and survey data, the method of estimating the result error is bigger, no authority for the China regional data.

At the same time, due to the lack of Mongolia, Pakistan, Uzbekistan observation data, the simulation of soil respiration also lack sufficient validation, simulation verification to China also need to be further strengthened. These are to be the next step work continued to improve and improve.

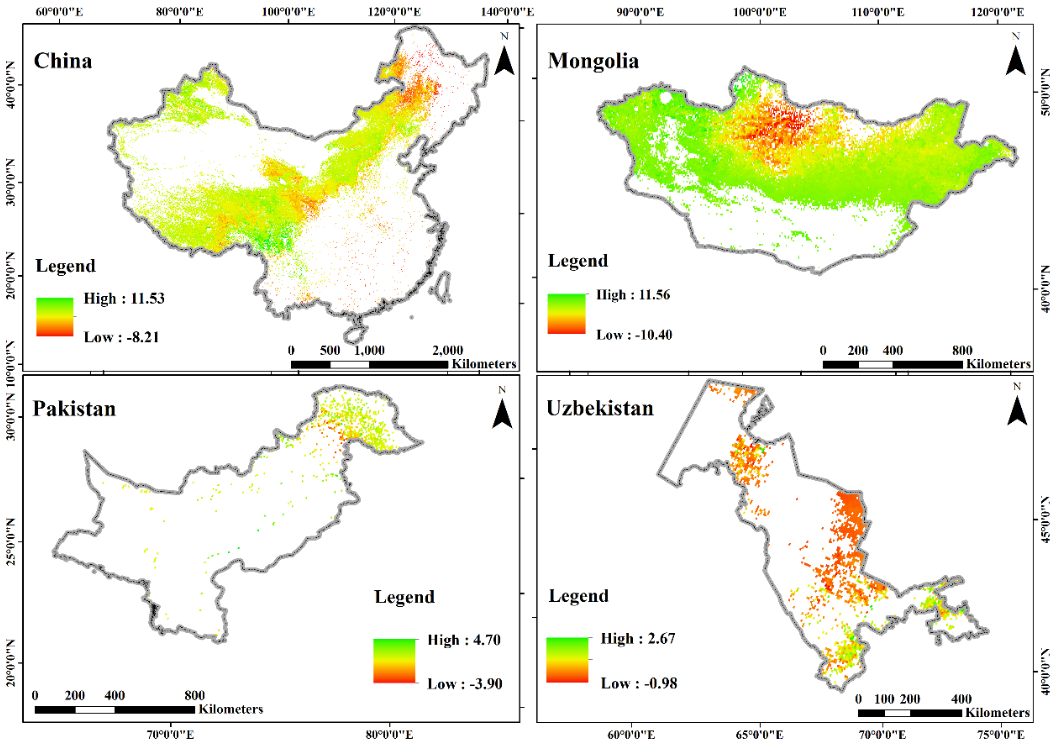

Figure 19 The changing trend of grassland NEP in these four countries (g C/m^2/year) (Yang, 2017)

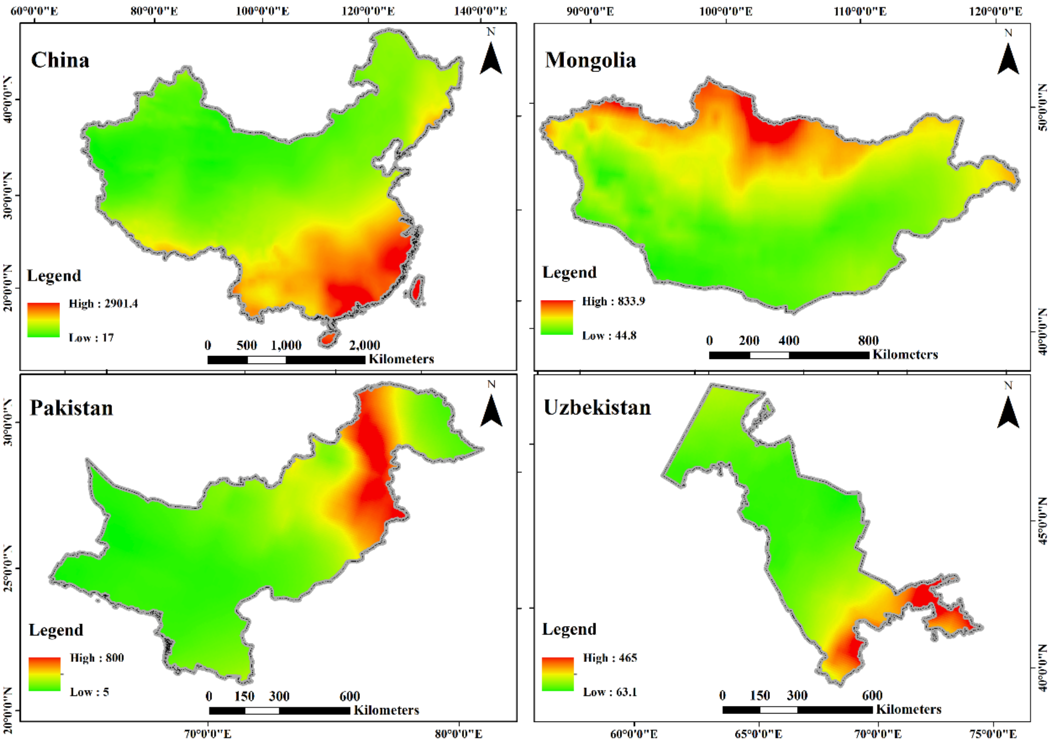

Figure 20 The distribution of precipitation in China, Mongolia, Pakistan and Uzbekistan (Yang, 2017)

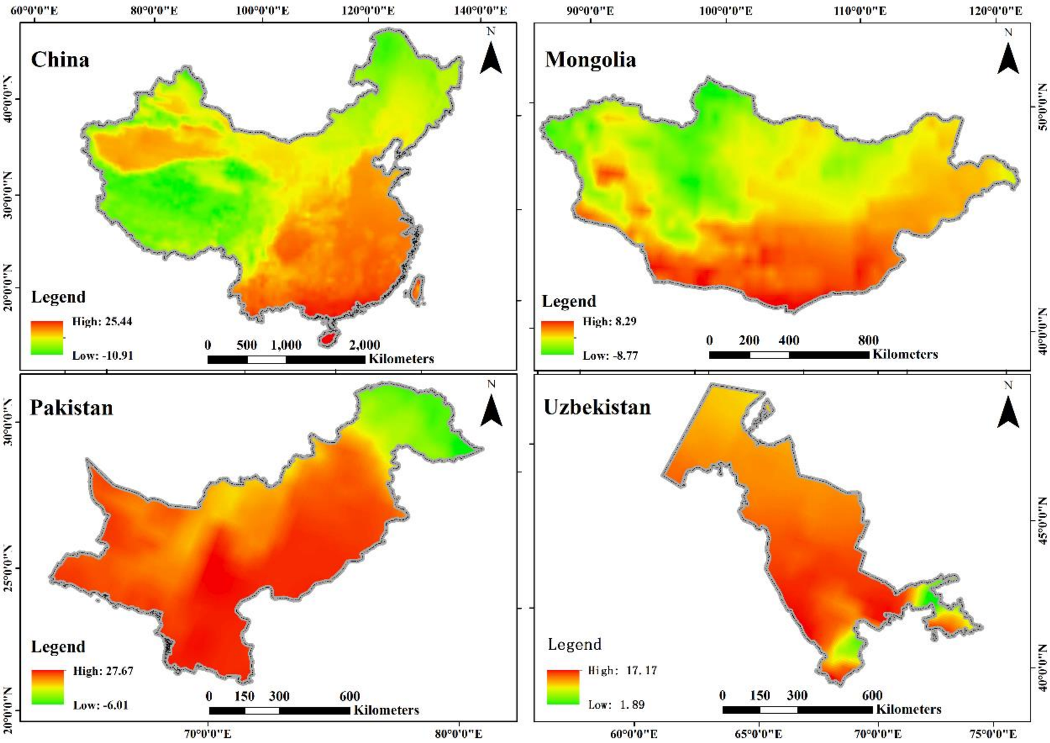

Figure 21 The distribution of temperature in China, Mongolia, Pakistan and Uzbekistan (Yang, 2017)

3.4. Assessing the Spatiotemporal Variations of Distribution, Extent and NPP of Terrestrial Ecosystems in Response to Climate Change from 1911 to 2000

In our previous paper (Gang , et al., 2013), we analyzed the distribution, extent and NPP of terrestrial ecosystems from 1911 to 2000, and came to the conclusion that consistently rising global temperature and altered precipitation patterns had exerted strongly influenced on spatiotemporal distribution and productivities of terrestrial ecosystems, especially in the mid/high latitude. The area of tundra & alpine steppe reduced significantly (5.43%), and were forced to head northward due to significant ascending temperature in northern hemisphere. In accordance, the global terrestrial ecosystems productivities increased by 2.09%. In general, effects of climate change on terrestrial ecosystems were deep and profound in 1911-2000, especially the latter half period. Key challenges for estimating grassland ecosystems vulnerability under varying temperature and precipitation changes lie in better recognizing how and to what extent the past climate change have affected the grassland ecosystems. To better clarify this issue, in this study, the distribution and shifts of grassland ecosystems as well as their NPP from 1910 to 2010 were evaluated. The correlation analysis between NPP dynamics and climate factors in the same period were also performed to reveal how climate changes have controlled the grassland productivity. The outcomes of this study do not only shed lights on how grassland ecosystems responded to climate change, but provide a basis for better grassland management. The results may be partly complement to IPCC report. Furthermore, methods used in this paper can serve as a guidance for regions lacking of collected data in past and future global change research.

The grassland ecosystems have long been affected by climate change, knowledge about how grassland ecosystems responded to climate change is still lacking. To evaluate how the climate change have affected the grassland ecosystems across the globe from 1910 to 2010, in this study, the spatiotemporal dynamic of distribution, shift ranges and net primary production (NPP) of grassland ecosystems were analyzed by using the modified comprehensive sequential classification system (CSCS) and the segmentation model. The results showed that consistently increasing temperature and altered precipitation patterns had exerted strongly influence on spatiotemporal distribution and productivities of grassland ecosystems, especially in the mid- and high latitude. The total area of grassland ecosystems widespread declined by 73.58 × 10^4 km^2 (1.42%) over the past 100 years. Only the distribution of tropical savannas expanded with 238.06 × 10^4 km^2 (12.36%), while areas of all the other grassland type decreased, the largest reduction was found in tundra & alpine steppe. During this period, most grasslands were forced to shift northwards due to the significant ascending temperature, particularly in the northern hemisphere. The longest and shortest shift distance was found both in the southern hemisphere, for the desert grassland shift 1289.75 km towards southwest, and the tundra & alpine steppe move towards northeast with 55.38 km. Meanwhile, the global grassland NPP showed an overall increasing trend with a rate of 745.52 Tg DW yr^{-1} (2.88%), within which tropical savannas contributed the most. By contrast, NPP of all the other grassland types declined during this period. Grassland NPP was more correlated with mean annual precipitation in comparison to mean annual temperature.

To assess the variations of distribution, extent and NPP of global natural vegetation in response to climate change in the period 1911-2000, and to provide a feasible method for global change research in regions where historical data collected/observed were difficult to be obtained. In this research, variations of spatiotemporal distributions of global potential natural vegetation (PNV) from 1911 to 2000 were analysed with the comprehensive sequential classification system (CSCS), and net primary production (NPP) of different ecosystems was evaluated with the Synthetic model, to determine the effect of climate change on the terrestrial ecosystems. The results showed that consistently rising global temperature and altered precipitation patterns had exerted strongly influenced on spatiotemporal distribution and productivities of terrestrial ecosystems, especially in the mid/high latitude. Ecosystems in temperate zones expanded and the areas of global deserts decreased as a consequence of climate variations. The mostly decreased vegetation was cold desert (18.79%), while the maximum increase (10.31%) was recorded on Savana. In addition, the area of tundra & alpine steppe reduced significantly (5.43%), and were forced to head northward due to significant ascending temperature in mid-and high latitude. In accordance, the global terrestrial ecosystems productivities increased by 2.09%, most of which was attributed to Savana (6.04%), tropical forest (0.99%) and temperate forest (5.49%), whereas the most NPP losses was found on cold desert (27.33%). NPP increase also presented latitudinal distribution, tropical zone, NPP of which amounted to more than a half of total NPP, was estimated to be the maximum increase with 1.32%, and followed by NPP in North Temperate Zone with 3.55%. At global scale, NPP showed a significant positive correlation with precipitation in comparison to mean annual temperature and biological temperature. In general, effect of climate change on terrestrial ecosystems was deep and profound in 1911-2000, especially the latter half period (Gang C. , 2015).

3.5. Assessing the impact of restoration-induced land conversion and management alternatives on net primary productivity in Inner Mongolian grassland, China

Using Inner Mongolia (IM) as a case study, we used MODIS NDVI data to estimate the vegetation coverage for assessing the current status of grassland, and calculated the changing trend of vegetation coverage from 2001 to 2010 to judge whether the grassland showed restoration trend or degradation trend. Net primary productivity (*NPP*) was selected as an indicator to measure the relative contributions of climate change and human activities. We used ArcGIS 9.3 software to analyse the spatial heterogeneity of vegetation dynamics and the contributions of the two factors by combining the biome boundaries of IM. Grassland was the most widespread vegetation in China and has a major influence on environmental quality and social-economic development. Accurate assessing of its dynamics as well as its relevance to climate change and human activities has attracted the attention of many researchers. In this paper, vegetation dynamics of the grassland in Inner Mongolia were studied by analyzing 10 years' (2001-2010) satellite observations of vegetation coverage. Potential *NPP* and the difference between potential and actual *NPP* were selected as indicators to assess the relative role of climate change and human activities in vegetation dynamics. The mean vegetation coverage of the total grassland area in Inner Mongolia was 0.37 in 2010, increasing gradually from the southwest to the northeast part of the region. During 2001-2010, 42.10% of the region's total grassland area tended to be restored, while 45.06% exhibited a degradation trend. Human activities were the dominant driving force responsible for 78.54% of the restoration process, while climate change only contributed 19.05%. However, in the degradation process, climate change nearly played a coequal role with human activities, contributing 40.50% and 55.69%, respectively (Mu, et al., 2014)**.**

3.6. Assessing the spatiotemporal dynamics of carbon balance of the terrestrial biosphere in response to climate change in 1911-2000

To assess how terrestrial ecosystems react to climate change at different scales in a long term, in this paper, the spatiotemporal variability of terrestrial carbon flux at global and continental scales were assessed and compared in the period 1911-2000. The 30-year running mean values results indicated that the terrestrial biosphere has been approximately neutral in 1911-1940 periods, and climate variability and change promoted absorbance of terrestrial carbon in 1941-1970 periods with 0.482 Pg C yr^{-1}, while in 1971-2000, the sink effect weakened with 0.239 Pg C yr^{-1}. Ecosystems in Europe and North America were estimated to have been absorbing carbon in the last 90 years. Savanna and temperate forest contributed the most to carbon uptake than other ecosystems, while most carbon release was induced by tropical forest. Ecosystems at northern mid-latitude north of the tropics have been sinks for atmospheric carbon, and the effect strengthened gradually in the past 90 years. By contrast, the South Temperate Zone appeared neutral for carbon in 1911-1970, while carbon accumulated significantly and amounted to 0.208 Pg C yr^{-1} in 1971-2000. The tropic zone appears to be a small net source of carbon in 1911-1940, and then carbon was accumulating in 1941-1970. However, in 1971-2000, a robust carbon source was formed. Due to the consistently rising global temperature and redistributed precipitation patterns, the distribution of terrestrial ecosystems changed with shrinking mid- and high latitude ecosystems, while expanding of ecosystems in temperate zones. Accordingly, the global terrestrial NPP increased during the past century, but it didn`t cause a substantial terrestrial carbon sink, for warming may enhance NPP, but also stimulates soil respiration. In general, the react of carbon flux of different terrestrial ecosystem varied a lot in response to climate change, and the generation or reversal of the terrestrial carbon sink caused by climate change itself may play a negative feedback to the climate system (Wang Z. , 2016)**.**

3.7. Assessing the Spatiotemporal Dynamic of Global Grassland Carbon Use Efficiency in Response to Climate Change from 2000 to 2013

Carbon use efficiency (CUE) mainly refers to the allocation of photosynthesized products by plants and is commonly used to measure the primary production of plants in terrestrial systems. To reveal whether the global grassland ecosystem is becoming more or less effective in storing carbon under climatic fluctuation, in this study, the annual CUE of grassland ecosystems was calculated from 2000 to 2013 based on the MODIS data. The spatiotemporal dynamics of grassland CUE and their correlations with climate variables were also investigated to reflect how ongoing climate variations are affecting grassland CUE at a global scale. The results showed that the highest and lowest value of CUE was recorded in closed scrublands with 53.93% and woody savannas with 46.51%, respectively. From 2000 to 2013, nearly 55.76% of grassland areas experienced increasing CUE, and most of these regions (44.33%) experienced non-significant increase. By contrast, regions experienced non-significant decrease accounted for 38.64% of total grassland areas, and mainly distributed in east of Australia and south of Africa. Regions showing significant and extremely significant decrease CUE accounted for 3.67 and 1.93% of total grassland areas, and mainly concentrated in the west of the Kgalagadi Basin and north of the Turan plain. During the period 2000 to 2013, the maximum increase of CUE

(0.251%/yr) was found in wood savannas, while the least increase (0.022%/yr) was observed in non-woody grasslands. The temporal dynamics of the grassland CUE were strongly controlled by temperature and precipitation. The areas of grassland CUE demonstrated a positive correlation with MAP and a negative correlation with MAT accounted for 68.68 and 68.81% of total grasslands, respectively. A warmer and drier condition would led to higher ecosystem respiration and lower net productivity, which would limit the capability of grassland ecosystems to store carbon (Wang Z. , 2016).

3.8. Several main innovations in the research methodology

1) This research paper improves the algorithm of the optimum temperature. This paper adopts vegetation growth temperature which is proposed to solve the method of upper and lower in NDVI corresponds to the maximum temperature and NDVI change rate corresponding to the largest temperature to determine the appropriate vegetation growth temperature of upper and lower limits. Then, based on suitable growth temperature range, calculated temperature and NDVI partial correlation relationships beside the influence of precipitation. Though the significance test, the maximum correlation coefficient of the corresponding temperature value is defined as the optimum temperature.
2) Maximum light energy utilization is one of the most important input parameters of CASA model, its value is different between different vegetation types. Previous study found that the ε_max was also affected by leaf area index, thus assuming maximum light energy utilization and vegetation index and leaf area index multiplicative factor relations, and inverse proportion. But this method has been used on small regions and China's grassland areas, and have achieved good results. In other areas and even the global scale has not been verified. Therefore, this article applied this method in the global grassland NPP simulation. Through the validation of the measured data, this method has been proved that has a good applicability on a global scale.
3) Among the influence factors of NPP in the grassland ecosystem research, research focuses on the impact of climate change trend of long-term average assessment ways, and less research focused on extreme weather events. At the same time, the research about drought mostly focused on the influence of forest ecosystem, few studies have been done on grassland ecosystem. And the study scale is small, lacking of large-scale comprehensive analysis. Therefore, this study used scPDSI drought index to study the effect of drought on global grassland NPP, helps to elucidate climate change especially extreme climate

influence on the grassland ecosystem carbon cycle process, and have important significance on disaster prevention and mitigation and adaptation countermeasures of extreme events.

4. Conclusions

4.1. Main Achievements from the project

Grasslands are among the largest biomes in the world, accounting for nearly 25% of the land surface on earth. Grasslands have many ecological functions, such as wind prevention, sand fixation, soil and water conservation, climate adjustment and air clearness. Grasslands significantly contribute to food security by providing food for ruminants, which are sources of meat and milk for human consumption. Due to the largest distribution, grassland ecosystems also play a key role in balancing the concentrations of global atmospheric greenhouse gases, reducing the effects of green-house gases through carbon storage and sequestration. With the global climate change and intensification of human activities, structures and functions of grassland ecosystems have been changing accordingly. Assessing the effects of climate change on the spatiotemporal distribution and dynamic of grassland ecosystems and driving factors do not only help to understand in the interactions of global change and grassland ecosystems, but provide baselines for grassland carbon cycle and global terrestrial carbon cycle assessment.

Based on global grassland as the main research object, we used the International Geosphere Biosphere Program (IGBP) to obtain the grassland area. Model simulation is the main research methods, as remote sensing and meteorological data was used to drive the model driven during the 1982-2008 period. Based on our researching works, our project had accomplished the following achievements:

- based on the CASA model, on the basis of the model parameters of the largest light energy utilization coefficient and temperature stress of the algorithm of optimum temperature was improved, using the improved CASA model to simulate the global grassland net primary productivity from 1982 to 2008, and the ground verifies the accuracy of the measured data of the improved model.
- to simulate the 1982-2008 global grassland Net primary productivity (NPP) the spatial distribution and its variation characteristics over time.

- based on the analysis of global temperature and precipitation from 1982 to 2008, we analyse the the spatial distribution and internal characteristic, explore the correlation between global grassland NPP and temperature and precipitation.
- using scPDSI drought index to analyses the global grassland drought occurred in 1982-2008 range and extent, through the analysis of global grassland scPDSI drought index characteristics and evolution of space and time, and study its impact on the global grassland NPP.
- the spatial distribution and variation of global grassland NPP was simulated in this study, a comparative analysis was conducted to detect the spatial differences of NPP which modelled by three model, and its correlation with climate factors was also performed.

4.2. Main Advances and Conclusions from the project

1) By our project, the spatial distribution of grassland NPP dynamic was represented in the four regions and the grassland NPP variation of these four regions were calculated from 2000 to 2013. The grassland NPP increased 859.63 Gg C year^{-1}, 306.9 Gg C year^{-1}, 49.4 Gg C year^{-1} in China, Mongolia and Pakistan, respectively. In Uzbekistan, the grassland NPP decreased by 9.4 Gg C year^{-1}. The trend of NPP variation was consistent with the change of grassland area in these four regions. Furthermore, our results had showed that the spatial trends of grassland NPP at different significance levels are not equal in the four regions. For example, Mongolia has the largest percentage of grassland with slight increase, which accounts for 64.93% of the grassland. Pakistan has the largest percentage of grassland with significant increase (17.81%) and extremely significant increase (14.68%) in the four regions. The largest percentage of grassland with slight decrease occurred in Uzbekistan, accounting for 60.93% of the grassland area.
2) In the project, the CASA model estimated that the biomass carbon storage was 1.47 Pg C, 0.44 Pg C, 0.03 Pg C, 0.03 Pg C in China, Mongolia, Pakistan and Uzbekistan, respectively. By contrast, the soil carbon storage was 29.25 Pg C, 13.86 Pg C, 0.46 Pg C, 0.29 Pg C in these four regions. The grassland carbon storage contained the biomass carbon storage and soil carbon storage. Among these four countries, the soil carbon storage accounted for most of the total carbon storage, and the proportions were all over 90%. As China had the largest areas of grassland, it had the most grassland carbon storage among the four countries. Mongolia had the second largest carbon storage. And, followed by Pakistan and Uzbekistan. It should be noted that our model results were close to the estimates made by Ma et al. (2016).

For instance, it was estimated that the biomass carbon storage was 1.61 Pg C and SOC storage was 29.37 Pg C using six methods (three spatial interpolation methods and three grassland classification methods) to estimate carbon storage of Chinese grasslands based on published data. Fang et al. (2010)'s estimation of biomass carbon and SOC storage also agreed with the results of our study.

3) The distribution of grassland NEP in China was presented in Figure 18. We can see from the figure that the general distribution characteristics of the grassland NEP higher from north to south, the central and northeast of China was low, the grassland NEP in Qinghai-Tibet Plateau was high. The carbon sources (NEP < 0) was mainly located in Sichuan Basin, northeast part of Inner Mongolia. The carbon sink (NEP > 0) was mainly distributed in the southeast of Tibetan. In Mongolia, the carbon sources (NEP < 0) was mainly located in the central and east of Mongolia. The carbon sink (NEP > 0) was mainly distributed in the Hovsgol. By contrast, the grassland is a weak carbon sinks in Pakistan. And the grassland in Uzbekistan was almost the carbon sinks. Through our researches, we found that the annual average grassland NEP in China was 0.01448 Pg C/year, which showed the grassland ecosystem absorb carbon dioxide from the atmosphere. In Mongolia, the grassland annual average NEP was negative value (-0.00725 Pg C/year), which explained that the grassland ecosystem released the carbon dioxide into the atmosphere. In Pakistan, the grassland annual average NEP was negative value (-0.00037 Pg C/year). Both the grassland in Mongolia and Pakistan are weak carbon source, and the Pakistan was even weaker when compared with the grassland NEP in Mongolia. In Uzbekistan, the annual average grassland NEP was 0.00139 Pg C/year.
4) Our study is based on CASA model, on the basis of the model parameters are maximum light energy utilization coefficient and temperature stress of the optimum temperature of the algorithm is improved, and by using the improved CASA model to simulate the grassland net primary productivity in the world during 1982 to 2008, and we used the measured data to assessment the accuracy of the improved model. Results show that the improved CASA model can be used in the estimating of grassland NPP simulation NPP value of correlation between measured values with the ground reached significant level (R2 = 0.77, P < 0.05).
5) Our study used improved CASA model to simulate the global spatial distribution of grassland NPP from 1982 to 2008. We found that the global total grassland NPP in an average of 24.73±0.27 Pg C /yr. The growth trend of global grassland NPP to present more significantly (P < 0.05) from 1982 to 2008, the growth trend of 0.0254 Pg C/yr. Using the piecewise linear regression model, the global grassland NPP from 1982 to 1982 showed significant growth

trend (P < 0.05), the annual growth rate of 0.0554 Pg C/yr, while show no significant downward trend from 1996 to 2008, annual growth rate of 0.0337 Pg C/yr. Analysis different grassland types, savannas has the highest average NPP, was 560.07 g C/m2/yr, followed by woody savannas, 474.45 g C/m2/yr, closed shrub land and non woody grassland were 328.58 and 237.78 g C/m2 /yr, and the lowest was open shrub land, 162.53 g C/m2/yr.

6) By analysing the space-time dynamic temperature and precipitation of global grassland, it is concluded that global average temperature of grassland presents ascendant trend during 1982-2008, and have a significant increase trend after 1995. And at the same time of the precipitation in 1982-1995, on the whole a decrease trend, the trend of decline is not significant. After 1995, the precipitation showed a rising trend of global grassland, and the increase of 1999-2006 trend is significant. Through the analysis of NPP and the internal correlation between temperature and precipitation, we found that the positive correlation between temperature and the NPP was 0.47 and negative correlation was 0.48; the positive correlation between precipitation and NPP of was 0.49, and the negative correlation was 0.43. Therefore, in terms of global scale, precipitation is the main climate factor of grassland NPP. In the area or regional scale, the temperature's influence on the grassland NPP will become more prominent.

7) By using scPDSI drought index, the paper analyzes the global grassland drought occurred in 1982-2008. Through the global grassland scPDSI features and evolution regularity of drought index, the results show that scPDSI drought index of the grassland has a good applicability. It can reveal the drought situation of global grassland and different grassland types. The trend of global grassland scPDSI drought index rise on the whole during 1982-2008, the average speed was 11.9%/10 a, especially in the 2004-2005 and 2008, the scPDSI drought index increased significantly. The drought area had a decreasing trend, and sizes of different grassland types of drought area as follows Savannas > Non woody grassland > closed shrublands > open shrublands > Woody savannas. Spatial distribution of drought occurred on different levels of spatial differentiation characteristics significantly. Through the study, global scPDSI drought index showed a trend of synchronous increase and decrease with grassland NPP during 1982-2008, namely the more severe drought year, the lower the NPP. Where the drought occurred more seriously, the NPP is also lower, and in the region of the drought degree is weakening, NPP also weakens. The scPDSI drought index of different grassland type and the change trend of NPP is synchronous, the increase or decrease performance of closed shrub land is more obvious. Through the analysis of the influence of grassland under

different level of drought area and the corresponding variation in NPP, shows that global grass drought happens the scope and degree of volatility during 1982-2008, and show the weakening trend on the whole, and t grassland NPP only have dropped affected by the drought during the 1992-1996.

8) Using the CASA model to simulate the spatial distribution of the global potential NPP grassland, the actual NPP and the NPP affected by human activities. Based on time series of the changing rate of these three NPP, established the quantitative evaluation of human and climate factors of the grassland NPP scene model. The results showed that 54.89% of the world's grassland NPP increase at a rate of about 1.76 gC/m^2 annually, compared with 45.1% of the grassland 0.54 gC/m^2 per year rate reduce, play a leading role in the grassland NPP climate change, the cause of global grassland NPP increase 64736.52 GgC, climate and human interaction is the main factors of grassland NPP reduce caused the reduction of the grassland NPP 4210.96 GgC. The correlation between rainfall and NPP was the highest in the climate factor, is the main climate factor decided the grassland NPP. Climate and human factors of influence on the grassland NPP quantitative simulation helps to meet the global ecosystem carbon cycle, so as to provide basis for improving grassland ecosystem management and decision making.

In summary, this project had simulated the spatial distribution of grassland net primary productivity and NEP and its temporal variation characteristics with the modified CASA model, and analyses the impacts of climate factors such as temperature, precipitation, and human activities on net primary productivity of grassland (Yang, 2017).

5. Future Directions

1) Due to the limited financial support obtained from APN, a large amount of in-kind data, models and resources were not utilised from the host and collaborative organizations in the development of the tool and undertaking field case study applications in other 3 countries.
2) Some of the case study applications are still in progress and need additional resources to complete those. The methodology, model and reviewing system developed in this project has broad applicability in more countries.
3) One of the potential future scientific researches is to expand the methodology and model to incorporate related issues such as husbandry and farm.
4) For wider use of the integrated system and results, it is highly important to develop good user-interface and technical and user guides.

5) To continue the research work and finish the future research objectives, we will need to continue the future works and get new 2017 -2018 funds from the APN.

6. References

Akiyama, T., & Kawamura, K. (2007). Grassland degradation in China: Methods of monitoring, management and restoration. *Grassland Science*(53), 1-17.

Chen, B., Zhang, X., Tao, J., Wu, J., Wang, J., Shi, P., . . . Yu, C. (2014). The impact of climate change and anthropogenic activities on alpine grassland over the Qinghai-Tibet Plateau. *Agricultural and Forest Meteorology, 189-190*, 11-18.

Fan, B., Luo, G., Hu, Z., Li, C., Han, Q., & Wang, Y. (2012). Land resource development and utilization in Central Asia. *Arid Land Geography, 35*, 928-937.

Foley, J., & Pollard, D. (2000). Incorporating dynamic vegetation cover within global climate models. *Ecological Applications, 10*, 1620-1632.

French, N. (1979). *Perspectives in grassland ecology: Results and applications of the US/IBP grassland biome study.* Springer-Verlag.

Gang , C., Zhou, W., Li, J., Chen, Y., Mu, S., Ren, J., & Groisman, P. Y. (2013). Assessing the spatiotemporal variation in distribution, extent and NPP of terrestrial ecosystems in response to climate change from 1911 to 2000. *PLoS ONE, 8*(11), e80394. doi:10.1371/journal.pone.0080394

Gang, C. (2015). *Quantitative assessment of the spatiotemporal variation of global grassland productivities and driving factors analysis in 1911-2011.* Nanjing University.

Gang, C., Zhou, W., Chen, Y., Wang, Z., Sun, Z., Li, J., . . . Odeh, I. (2014). Quantitative assessment of the contributions of climate change and human activities on global grassland degradation. *Environmental Earth Sciences, 72*, 4273-4282.

Gao, Y., Xu, Z., Qiao, W., Wang, C., Zhan, Z., Chen, L., . . . Ran, Q. (2013). Vegetation net primary productivity and its response to climate change during 2001-2008 in the Tibetan Plateau. *Science of the Total Environment, 72*, 356-362.

Han, J. G., Zhang, Y. J., Wang, C. J., Bai, W. M., Wang, Y. R., Han, G. D., & Li, L. H. (2008). Rangeland degradation and restoration management in China. *The Rangeland Journal, 30*, 233-239.

Herrmann, S. M., Anyamba, A., & Tucker, C. J. (2005). Recent trends in vegetation dynamics in the African Sahel and their relationship to climate. *Global Environmental Change, 15*, 394-404.

Horion, S., Cornet, Y., Erpicum, M., & Tychon, B. (2013). Studying interactions between climate variability and vegetation dynamic using a phenology based approach. *International Journal of Applied Earth Observation and Geoinformation, 20*, 20-32.

Intergovernmental Panel on Climate Change. (2014). *2014: Climate Change 2013 - The Physical Science Basis.* Cambridge University Press.

Li, B. (1997). The Rangeland Degradation in North China and Its Preventive Strategy. *Scientia Agricultura Sinica*.

Lieth, H. (1975). *Modeling the Primary Productivity of the World.* Springer Berlin Heidelberg.

Lieth, H., & Box, E. (1972). Evapotranspiration and primary productivity. *Publications in Climatology, 25*, 37-46.

Liu, Y., & Zha, Y. (2004). Assessment of grassland degradation near Lake Qinghai, West China, using Landsat TM and in situ reflectance spectra data. *International Journal of Remote Sensing, 25*, 4177-4189.

Lu, D., Batistella, M., Mausel, P., & Moran, E. (2007). Mapping and monitoring land degradation risks in the Western Brazilian Amazon using multitemporal Landsat TM/ETM+ images. *Land Degradation and Development, 18*, 41-54.

Ma, T., Zhou, C., & Pei, T. (2012). Simulating and estimating tempo-spatial patterns in global human appropriation of net primary production (HANPP): A consumption-based approach. *Ecological Indicators, 23*, 660-667.

Mu, S., Li, J., Chen, Y., Ju, W. M., Zou, X. L., & Odeh, I. (2014). Grassland dynamics in response to climate change and human activities in Inner Mongolia, China between 1985-2009. *The Rangeland Journal, 35*(3), 315-329.

Mu, S., Yang , H., Li, J., Chen, Y., Gang, C., Zhou, W., & Ju, W. (2013). Spatio-temporal dynamics of vegetation coverage and its relationshop with climate factors in Inner Mongolia, China. *Journal of Geographical Sciences, 23*, 231-246.

Mu, S., Zhou, S., Chen, Y., Li, J., Ju, W., & Odeh, I. (2013). Assessing the impact of restoration-induced land conversion and management alternatives on net primary productivity in Inner Mongolian grassland, China. *Global and Planetary Change, 108*, 29-41.

O'Mara, F. P. (2012). The role of grasslands in food security and climate change. *Annals of Botany, 110*, 1263-1270.

Rojstaczer, S., Sterling, S. M., & Moore, N. J. (2001). Human appropriation of photosynthesis products. *Science, 294*, 2549-2552.

Scurlock, J. M., & Hall, D. O. (1998). The global carbon sink: a grassland perspective. *Global Change Biology, 4*, 229-233.

Sekiyama, A., Takeuchi, W., & Shimada, S. (2014). Detection of grassland degradation using MODIS data in Mongolia (Desert Technology 11 International Conference). *Journal of Arid Land Studies, 24*, 175-178.

Wang, T., Sun, J., Han, H., & Yan, C. (2012). The relative role of climate change and human activities in the desertification process in Yulin region of Northwest China. *Environmental Monitoring Assessment, 184*, 7165-7173.

Wang, Z. (2016). *The carbon storage accounting of global grassland ecosystem in response to climate change.* Nanjing University.

Wessels, K. J., Prince, S. D., Malherbe, J., Small, J., Frost, P. E., & VanZyl, D. (2007). Can human-induced land degradation be distinguished from the effects of rainfall variability? A case study in South Africa. *Journal of Arid Environments, 68*, 271-297.

Xu, D. Y., Kang, X. W., Liu, Z. L., Zhuang, D. F., & Pan, J. J. (2009). Assessing the relative role of climate change and human activities in sandy desertification of Ordos region, China. *Science in China, 52*, 855-868.

Xu, D., Kang, X. W., Liu, Z. L., Zhuang, D. F., & Pan, J. J. (2010). Multi-scale quantitative assessment of the relative roles of climate change and human activities in desertification - A case study of the Ordos Plateau, China. *Journal of Arid Environments, 74*, 498-507.

Xu, W., Gu, S., Zhao, X. Q., Xiao, J., Tang, Y., Fang, J., . . . Jiang, S. (2011). High positive correlation between soil temperature and NDVI from 1982 to 2006 in alpine meadow of the Three-River Source Region on the Qinghai-Tibetan Plateau. *International Journal of Applied Earth Observation and Geoinformation, 13*, 528-535.

Yang, Y. (2017). *Quantitative assessment of the NPP, NEP and carbon sinks of four countries and global grassland and driving factors analysis using modified CASA model.* Nanjing University.

Yeh, E. T. (2005). Green governmentality and pastoralism in Western China: Converting pastures to grasslands. *Nomadic Peoples, 9*, 9-30.

Ykhanbai, H., Bulgan, E., Beket, U., Vernooy, R., & Graham, J. (2015). Reversing grassland degradation and improving herders' livelihoods in the Altai Mountains of Mongolia. *Mountain Research and Development, 24*, 96-100.

Yong-Zhong, S., Yu-Lin, L., Jian-Yuan, C., & Wen-Zhi, Z. (2005). Influences of continuous grazing and livestock exclusion on soil properties in a degraded sandy grassland, Inner Mongolia, Northern China. *CATENA, 59*, 267-278.

Zhang, C., Wang, X., Li, J., & Hua, T. (2011). Roles of climate changes and human interventions in land degradation: a case study by net primary productivity analysis in China's Shiyanghe Basin. *Environmental Earth Sciences, 64*, 2183-2193.

Zheng, Y. R., Xie, Z. X., Robert, C., Jiang, L. H., & Shimizu, H. (2015). Did climate drive ecosystem change and induce desertification in Otindag sandy land, China over the past 40 years? *Journal of Arid Environments, 64*, 523-541.

Zhou, W., Gang, C., Zhou, F., Li, J., Dong, X., & Zhao, C. (2015). Quantitative assessment of the individual contribution of climate and human factors to desertification in northwest China using net primary productivity as an indicator. *Ecological Indicators, 48*, 560-569.

Zhou, W., Gang, C., Zhou, L., Chen, Y., Li, J., Ju, W., & Odeh, I. (2014). Dynamic of grassland vegetation degradation and its quantitative assessment in the northwest China. *Acta Oecologica, 55*, 86-96.

7. Appendix

7.1. Appendix 1. List of Young Scientists of our team in four countries in 2013-2017*

№	Name	Affiliation	Role	Output	Time line
1	Yue YANG	Doctor, Nanjing University	Project collaborator	Report Policy formulation Journal paper	2016 January to December 2017
2	Ying ZHANG	Lecture, Nanjing University	Environmental & grassland works and policy expert	Sampling analysis Journal paper	2016 January to December 2017
3	Zhao-qi WANG	Doctor, Nanjing University	Fieldwork works, experiments, sampling analysis	Journal paper Result report	2016 January to December 2017
4	Yi-zhao CHEN	Doctor, Nanjing University	Remote sensing analysis and grassland works	Web data base Design Journal paper	2016 January to December 2017

5	Cheng-cheng GANG	Lecture, Nanjing University	Grassland works and Simulation of potential erosion	Journal paper Degradation analysis	2016 January to December 2017

*contact: jili2008@nju.edu.cn

7.2. Appendix 2: Outputs and outcomes of this project in 2013-2017

No.	Outputs	Outcomes
1	Create a multidisciplinary team and website.	The team includes 4 experts from developing countries and 5 experts from developed countries.
2	May 29 - June 2. 2013: Our team had held the international meeting for four countries in Nanjing University of China.	A total of 46 participants, 10 experts of our project team have trained 8 young scientists and 28 students.
3	June 3 - June 8. 2013: Our team had investigated and toured the four-country international works in inner-Mongolia grassland in China.	Includes 6 experts and 12 students.
4	The published papers in first year.	Includes 10 Chinese papers, 6 English papers and 1 working report.
5	April 7-12, 2014: Our team had taken part in the MAIRS conference in Beijing in China.	Includes 10 representatives, and 4 of them had given a speech.
6	June 19 - June 24, 2014: Our team had investigated and toured the four-country international works in inner-Mongolia grassland in China.	6 experts and 12 students participated in Inner Mongolia grassland surveys.
7	June 25-June 29, 2014: Our team had held the international meeting in Xilinhot City in China.	8 experts of our project team have trained 48 young scientists and students.
8	The published papers in second year.	Includes 6 Chinese papers, 6 English papers and 1 working report.
9	April 13, 2017: We have held the working summary meeting in Beijing.	Includes 6 experts, in which 2 is form China, 2 is from America, 1 is from Mongolia and 1 is from Pakistan.
10	The published papers in third year.	Includes 10 Chinese papers, 8 English papers, 1 working report, 1 financial report and 1 technical report.
11	Graduate student in 3 years (Master, PhD).	Includes 6 Masters, 12 PhD and 2 post doctorates.
12	The published works in 2016.	1 book.
13	Access to Chinese government support.	2 projects.
14	Access to Australia government support.	1 project.
15	Support for international organizations.	1 Future Climate Change Scenario Report.
16	Support for IPCC 4.0	1 technical report.
17	The global grassland is divided into 4 broad categories, 42 categories.	Constructed 1 global grassland quantitative classification system.

18	We have improved CASA and LPA models.	Constructed 2 new grassland NPP valuation models.
19	We propose a new approach to quantitatively estimate grassland degradation using grassland productivity, grassland coverage, and taint index.	1 new method of grassland degradation monitoring.
20	1 set of grassland carbon source, sink quantitative estimation and verification system was constructed from soil - grass ecosystem.	We have obtained a lot of research data, theoretical results and published 23 scientific peer-reviewed papers from our team in 2013-2017.